Electron-Rich Piano-Stool Iron *σ*-Acetylides Bearing a Functional Aryl Group. Synthesis and Characterization of Iron(II) and Iron(III) Complexes†

Raphaël Denis,‡ Loïc Toupet,§ Frédéric Paul,*,‡ and Claude Lapinte*,‡

Organométalliques et Catalyze: Chimie et Electrochimie Moléculaire, UMR CNRS 6509, and Groupe Matière Condensée et Matériaux, UMR 6626, Université de Rennes 1, Campus de Beaulieu, 35042 Rennes Cedex, France

Received April 18, 2000

The synthesis and characterization of a family of *para*-functionalized complexes **3a**−**k**, [(η^2-dppe)(η^5-C_5Me_5)Fe(C≡CC_6H_4X)] (dppe = 1,2-(diphenylphosphino)ethane; X = NO_2, CN, CF_3, F, Br, H, Me, ^{t}Bu, OMe, NH_2, NMe_2), is reported. Most of the complexes were obtained in fair yields from the terminal iron acetylide complex [(η^2-dppe)(η^5-C_5Me_5)Fe(C≡CH)] (**1**) using a palladium/copper-catalyzed coupling reaction. The complex **3j**, with a strongly electron releasing NH_2 group, was synthesized by the more classical vinylidene route. The corresponding thermally stable radical cations could be generated in solution by addition of [(η^5-$C_5H_5)_2Fe^+$][PF_6^-] from **3a**−**k** and characterized by infrared spectroscopy. Selected examples of these iron(III) salts (**3a**, X = NO_2; **3f**, X = H; **3j**, X = NH_2) were isolated and more completely characterized by Mössbauer spectroscopy. Crystal structures were determined for (η^2-dppe)(η^5-C_5Me_5)Fe[C≡C-1,4-(C_6H_4)-NO_2] (**3a**), (η^2-dppe)(η^5-C_5Me_5)Fe(C≡C-1,4-(C_6H_4)-CN] (**3b**), (η^2-dppe)(η^5-C_5Me_5)Fe[C≡C−(C_6H_5)] (**3f**), and [(η^2-dppe)(η^5-C_5Me_5)Fe{C≡C-1,4-(C_6H_4)NO_2}$^+$][PF_6^-] (**3a**$^+$$PF_6^-$).

Introduction

Organometallic architectures incorporating metal atoms in organic π networks have given rise to a great deal of interest, owing to their promise for the elaboration of new molecular materials.[2−16] In addition, discrete molecules also constitute fascinating objectives, in order to understand the unusual properties that arise from the intimate combination of metal atoms with unsaturated ligands. Notably, such knowledge appears to be of use in the field of molecular-scaled electronics.[17] In this connection, we have studied several polynuclear organoiron compounds of various geometries, where electroactive (η^2-dppe)(η^5-C_5Me_5)Fe units are linked together, either (i) directly through polyynic bridges or (ii) via a central organic spacer by means of an ethynyl bridge. Depending on the redox state of the molecule and depending on its structure, electron transfer, magnetic-exchange coupling, or both interactions can take place between the remote metallic termini.[18] Among the compounds investigated, architectures based on a central aromatic core are particularly interesting, since tuning of the electronic properties appears feasible, depending on the geometry.[19−22] In these complexes, the nature of the electronic interaction between the metallic nuclei in a given redox state and the bridging ligand appears to determine the resulting electronic or magnetic properties exhibited by the polynuclear assembly.[7,18] Now, to complement these investigations, we have undertaken an extensive study of the mononuclear iron alkynyl complexes (η^2-dppe)(η^5-C_5Me_5)Fe(C≡C-C_6H_4X) (**3a**−**k**), simple model compounds that are able to unravel the nature of the bonding between the central diethynylaryl core and the terminal iron centers.

† This article will be complemented by theoretical calculations in a following paper.[1]

‡ UMR CNRS 6509: Organométalliques et Catalyse.

§ UMR 6626: Groupe Matière Condensée et Matériaux.

(1) Paul, F.; Lapinte, C.; Costuas, K.; Halet, J.-F. Work in progress.
(2) Chisholm, M. H. *Angew. Chem., Int. Ed. Engl.* **1991**, *30*, 673−674.
(3) Beck, W.; Niemer, B.; Wieser, M. *Angew. Chem., Int. Ed. Engl.* **1993**, *32*, 923−949.
(4) Lang, H. *Angew. Chem., Int. Ed. Engl.* **1994**, *33*, 547−550.
(5) Akita, M.; Moro-Oka, Y. *Bull. Chem. Soc. Jpn.* **1995**, *68*, 420−432.
(6) Long, N. J. *Angew. Chem., Int. Ed. Engl.* **1995**, *34*, 21−38.
(7) Manna, J.; John, K. D.; Hopkins, M. D. *Adv. Organomet. Chem.* **1995**, *38*, 80−154.
(8) Ward, M. D. *Chem. Ind.* **1996**, *15*, 568−573.
(9) (a) Bunz, U. H. F. *Angew. Chem., Int. Ed. Engl.* **1996**, *35*, 969−971. (b) Bunz, U. H. F.; Enkelmann, V. *Organometallics* **1994**, *13*, 3823−3835.
(10) Barigelletti, F.; Flamigni, L.; Collin, J.-P.; Sauvage, J.-P. *Chem. Commun.* **1997**, 333−338.
(11) Bruce, M. I. *Coord. Chem. Rev.* **1997**, *166*, 91−119.
(12) Ziessel, R.; Hissler, M.; El-gayhouri, A.; Harriman, A. *Coord. Chem. Rev.* **1998**, *178−180*, 1251−1298.
(13) Yam, V. W.-W.; Lo, K. K.-W.; Wong, K. M.-C. *J. Organomet. Chem.* **1999**, *578*, 3−30.
(14) Schwab, P. F. H.; Levin, M. D.; Michl, J. *Chem. Rev.* **1999**, *99*, 1863−1933.
(15) Martin, R. E.; Diederich, F. *Angew. Chem., Int. Ed.* **1999**, *38*, 1351−1377.
(16) Ziessel, R. *Synthesis* **1999**, 1839−1865.

(17) In line with a recent trend,[15] we feel that this definition is more suited than the general term "molecular electronics", which also includes the notion of "molecular-based materials for electronics".

(18) Paul, F.; Lapinte, C. *Coord. Chem. Rev.* **1998**, *178/180*, 427−505.
(19) Le Narvor, N.; Lapinte, C. *Organometallics* **1995**, *14*, 634−639.
(20) Weyland, T.; Lapinte, C.; Frapper, G.; Calhorda, M. J.; Halet, J.-F.; Toupet, L. *Organometallics* **1997**, *16*, 2024−2031.
(21) Weyland, T.; Costuas, K.; Mari, A.; Halet, J.-F.; Lapinte, C. *Organometallics* **1998**, *17*, 5569−5579.
(22) Weyland, T.; Costuas, K.; Halet, J.-F.; Lapinte, C. *Organometallics*, in press.

10.1021/om000325o CCC: $19.00 © 2000 American Chemical Society
Publication on Web 09/09/2000

Downloaded by NORTH CAROLINA CONSORTIUM on June 29, 2009
Published on September 9, 2000 on http://pubs.acs.org | doi: 10.1021/om000325o

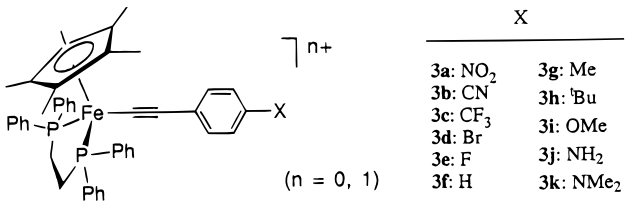

While the original synthetic access to several iron(II) phenylethynyl complexes by Pd/Cu catalysis has previously been communicated,[23] we now report the synthesis of the complete family (**3a**−**k**) and its characterization. We also report on the oxidized iron(III) counterparts **3a**$^+PF_6^-$−**3k**$^+PF_6^-$ and discuss the electronic structure of the alkynyl linker, which depends on the oxidation state of the iron center.

Results

Synthesis of the Neutral Complexes. While the unsubstituted complexes **3f** and **3f**$^+PF_6^-$ were known (X = H),[24,25] all other neutral Fe(II) acetylide complexes are new. Most of them have been synthesized by a Pd/Cu-catalyzed cross coupling reaction,[23] which has also been extended by us to heterocylic aryl bromides.[26] A similar "metalla-Sonogashira" reaction (Scheme 1) was independently developed and used by Bruce et al.[27] However, with electron-rich metallaalkynyls as in our case, the cornerstone of this synthetic approach rests in the recovery of the organometallic product in a pure form. Indeed, chromatographic purification of the products proved detrimental in several cases, and other means had to be devised to isolate the compounds in a pure state. Most often (**3a**−**g**), extraction in toluene and filtration on Celite followed by washings with cold *n*-pentane and acetonitrile fractions proved satisfactory. However, in some cases (**3h**,**i**,**k**) this procedure was not adapted and the product had to be purified by an alternative method based on an oxidation−reduction cycle (see the Experimental Section), which of course decreased the yield of isolated product.

The coupling conditions are derived from the Sonogashira reaction.[28] Typically, in diisopropylamine in the presence of 5% of the palladium(II) catalyst and 10% copper iodide, the desired coupled product (**3a**−**h**) can be isolated from the terminal iron alkynyl **1** in good yields with most of the substituted aryl bromides tested (**2a**−**h**). Expectedly, the reaction proceeds more and more sluggishly when the electron-releasing power of the substituent increases. This results in longer reaction times, higher reaction temperatures, and periodic catalyst renewal (see the Experimental Section), as for **3h**,**i**, where relatively harsh conditions had to be used for the coupling to proceed. With the strongly electron-donating NMe_2 substituent (**2k**), even under such drastic conditions, the desired complex (**3k**) was isolated admixed with several other unknown organoiron species, the latter resulting possibly from side reactions of **1** or **3k**. Complex **3k** could also not be isolated pure after the redox purification procedure but remained contaminated with 5−10% (^{31}P NMR) of a single unidentified complex. In the case of **2g**,**i**, the use of the corresponding aryl iodides did apparently slightly improve both the yield and the coupling rate. As a consequence, *p*-iodoanisole was preferred as a coupling partner for **1** in the reported synthesis of **3i**. Thus, owing to the easy synthetic access to complex **1** and to the commercial availability of the substituted aryl bromides **2a**−**k**, the catalytic Sonogashira-like approach constitutes a versatile synthetic route toward electron-rich iron alkynyls possessing strong to moderate electro-attracting substituents. It is particularly attractive in the case of electron-withdrawing substituents on the aryl bromide, since it offers an interesting alternative to the classical vinylidene route depicted in Scheme 2. The latter is more appropriate to substrates possessing strongly electron-releasing substituents on the aryl ring.[23,24] Accordingly, this route was used to synthesize the complex **3j** (X = NH_2) needed to complement our family. It requires two steps in addition to these devoted to the synthesis of the phenyl-substituted terminal alkynyl reactant, here the (4-aminophenyl)ethynyl group.[29]

Scheme 1

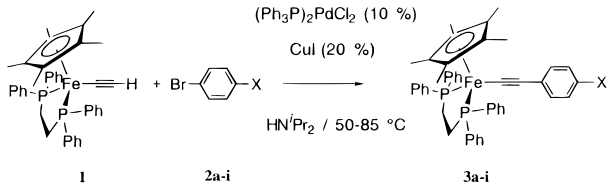

(**2-3a**: NO_2; **2-3b**: CN; **2-3c**: CF_3; **2-3d**: Br; **2-3e**: F; **2-3f**: H; **2-3g**: Me; **2-3h**: ^{t}Bu; **2-3i**: OMe)

Scheme 2

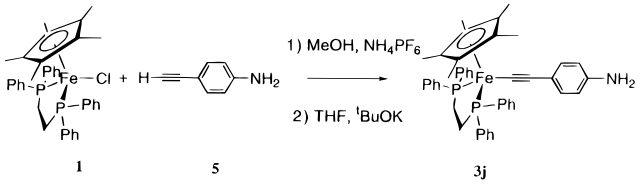

Characterization of the Neutral Complexes. The neutral complexes were characterized by the usual spectroscopy and high-resolution LSI mass spectrometry, while the X-ray data obtained for **3a**,**b**,**f** and **3a**$^+PF_6^-$ also confirm the proposed structures (Figures 1−4). Satisfactory elemental analyses were also obtained in selected cases (X = NO_2, CN, CF_3, ^{t}Bu, OMe, NH_2). Except for **3k**, all complexes were spectroscopically pure, as exemplified by the observation of a single peak in ^{31}P NMR, clean and sharp ^{1}H and ^{13}C NMR spectra, and voltammograms exhibiting oxidation waves attributable to a single redox-active species (Table 2).

The relevant NMR data are in line with the usual features expected for such complexes.[18,24,30] Notably, in ^{13}C NMR, the alkynyl α-carbon atoms of **3a**−**j** always

(23) Denis, R.; Weyland, T.; Paul, F.; Lapinte, C. *J. Organomet. Chem.* **1997**, *545/546*, 615−618.
(24) Connelly, N. G.; Gamasa, M. P.; Gimeno, J.; Lapinte, C.; Lastra, E.; Maher, J. P.; Le Narvor, N.; Rieger, A. L.; Rieger, P. H. *J. Chem. Soc., Dalton Trans.* **1993**, 2775−2578.
(25) Bitcon, C.; Whiteley, M. W. *J. Organomet. Chem.* **1987**, *336*, 385−392.
(26) Le Stang, S.; Lenz, D.; Paul, F.; Lapinte, C. *J. Organomet. Chem.* **1998**, *572*, 189−192.
(27) Bruce, M. I.; Ke, M.; Low, P. J.; Skelton, B. W.; White, A. H. *Organometallics* **1998**, *9*, 3539−3549.
(28) Sonogashira, K.; Tohda, Y.; Hagihara, N. *Tetrahedron Lett.* **1975**, *50*, 4467−4470.
(29) Lavastre, O.; Ollivier, L.; Dixneuf, P. H.; Sinbandhit, S. *Tetrahedron* **1995**, *52*, 5495−5504.

Downloaded by NORTH CAROLINA CONSORTIUM on June 29, 2009
Published on September 9, 2000 on http://pubs.acs.org | doi: 10.1021/om000325o

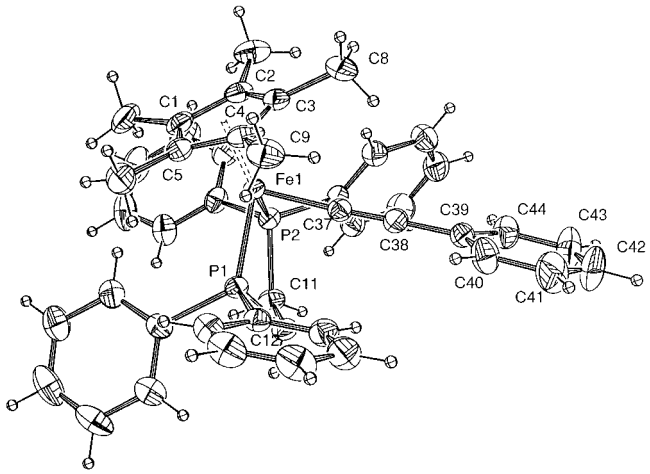

Figure 1. Molecular structure of (η^2-dppe)(η^5-C_5Me_5)Fe-(C≡C)-1,4-(C_6H_5) (**3f**·C_5H_{12}).

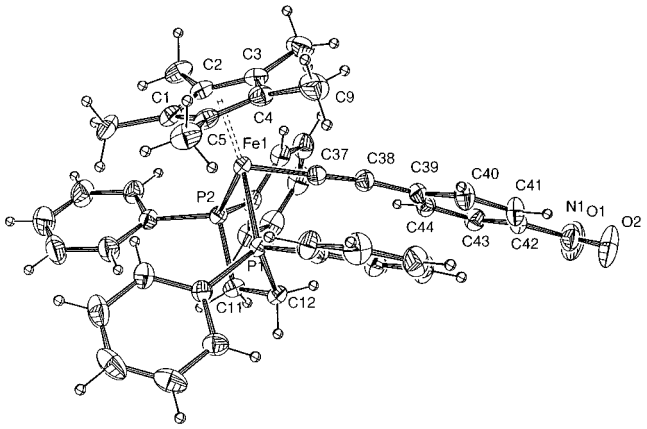

Figure 2. Molecular structure of (η^2-dppe)(η^5-C_5Me_5)Fe-(C≡C)-1,4-(C_6H_4)NO_2 (**3a**).

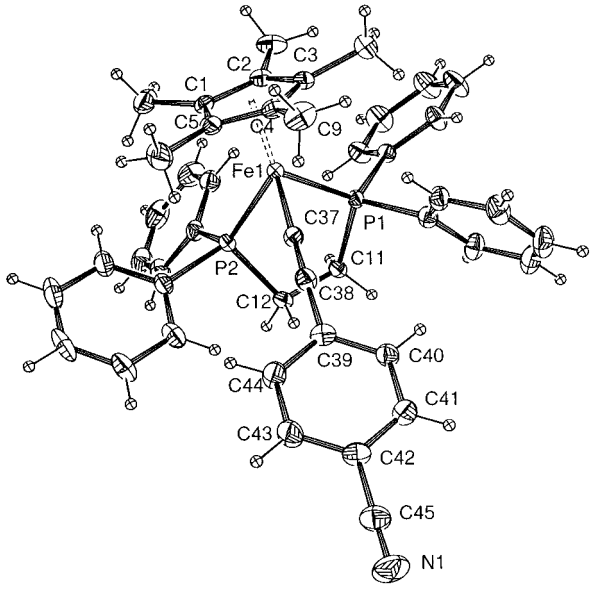

Figure 3. Molecular structure of (η^2-dppe)(η^5-C_5Me_5)Fe-(C≡C)-1,4-(C_6H_4)CN (**3b**).

appear coupled to the two phosphorus atoms of the dppe ligand with a $^3J_{PC}$ coupling constant of ca. 40 Hz. In some cases, this characteristic signal was hidden by other signals. Nevertheless, except for **3e**,**k**, this signal could be firmly located when a pulse sequence allowing only the quaternary carbons to be detected was used. On the other hand, the $^4J_{PC}$ coupling of ca. 3 Hz on the β-carbon atom is not always resolved, but since these signals do usually show up in a narrow spectral range, they could be identified each time as well.[31] Finally, it is worth pointing out that the ^{31}P NMR shift spans a very narrow range between 100 and 102 ppm for the entire family (**3a**−**k**). Electron-attracting substituents result in a slight shielding of the signal relative to unsubstituted **3f**, while the opposite is observed for electron-donating ones. The limited range of the shifts indicates, however, that the influence of the remote *para* substituent is only weakly sensed by the phosphorus nuclei, consistent with the data available for other functional phenylacetylide complexes.[32] A similar behavior can be observed for the ^{1}H NMR singlet of the

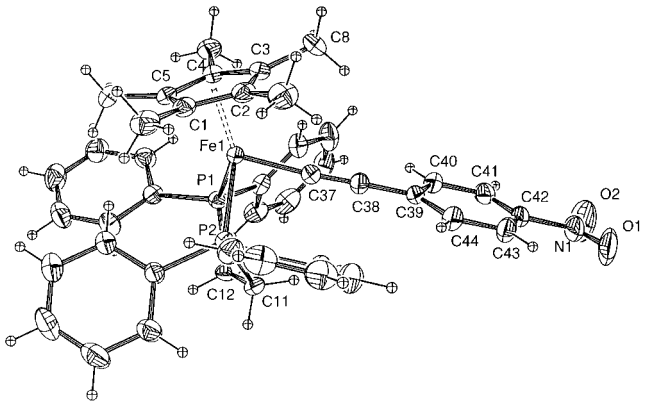

Figure 4. Molecular structure of [(η^2-dppe)(η^5-C_5Me_5)Fe-(C≡C)-1,4-(C_6H_4)NO_2^+][PF_6^-] (**3a**$^+PF_6^-$·$C_4H_{10}O$).

Table 1. Infrared Data for Selected Complexes in CH_2Cl_2 Solution[a] (cm^{-1})

compd	$\nu_{C\equiv C}$ neutral	$\nu_{C\equiv C}$ oxidized[b]	$\Delta\nu_{C\equiv C}$[c]
[Fe]C≡C(C_6H_4)NO_2 (**3a**)	2036	2038	+2
	2008		+30
[Fe]C≡C(C_6H_4)CN (**3b**)[d]	2048	not obsd	
	2025		
[Fe]C≡C(C_6H_4)CF_3 (**3c**)	2050	not obsd	
	2030 (sh)		
[Fe]C≡C(C_6H_4)Br (**3d**)	2054	2017	−37
		1991	−63
[Fe]C≡C(C_6H_4)F (**3e**)	2057	2005	−52
[Fe]C≡C(C_6H_5) (**3f**)	2053	2021	−32
		1988	−65
[Fe]C≡C(C_6H_4)CH_3 (**3g**)	2056	1994	−62
[Fe]C≡C(C_6H_4)^{t}Bu (**3h**)	2053	1996	−57
[Fe]C≡C(C_6H_4)OMe (**3i**)	2058	1988	−70
[Fe]C≡C(C_6H_4)NH_2 (**3j**)	2060	1988 (sh)	−72
		1962	−98
[Fe]C≡C(C_6H_4)NMe_2 (**3k**)	2056	1962	−94

[a] Solid-state $\nu_{C\equiv C}$ values obtained in Nujol mulls for isolated complexes are given in the Experimental Section. [b] Apart from **3a**$^+$ PF_6^-, **3f**$^+$ PF_6^-, and **3j**$^+$ PF_6^-, these values were obtained from Fe(III) acetylides generated in situ using [(η^5-$C_5H_5)_2Fe^+$][PF_6^-]. [c] Neutral vs oxidized $\nu_{C\equiv C}$ difference. [d] For these compounds the $\nu_{C\equiv N}$ signals are also observed at 2217 and 2228 cm^{-1} in CH_2Cl_2 solutions for, respectively, the neutral and oxidized complexes.

(30) Le Stang, S.; Paul, F.; Lapinte, C. *Inorg. Chim. Acta* **1999**, *291*, 403−425.

(31) The ^{13}C signal at 143.6 ppm in **3a** attributed to the β-alkynyl carbon in our previous communication has been revised (see the Experimental Section).[23]

Downloaded by NORTH CAROLINA CONSORTIUM on June 29, 2009
Published on September 9, 2000 on http://pubs.acs.org | doi: 10.1021/om000325o

Table 2. Electrochemical Data for Selected Complexes

compd	ΔE_p	E_0[a]	i_c/i_a	ref
[Fe]C≡C(C_6H_4)NO_2 (**3a**)	0.07	−1.28	1	this work
	0.12	−0.02	1	
[Fe]C≡C-*p*-(C_6H_4N) (**4a**)	0.09	−0.03	1	30
[Fe]C≡C(C_6H_4)CN (**3b**)	0.08	−0.05	1	this work
[Fe]C≡C(C_6H_4)CF_3 (**3c**)	0.075	−0.08	1	this work
[Fe]C≡C-*o*-(C_6H_4N) (**4c**)	0.09	−0.08	1	30
[Fe]C≡C-*m*-(C_6H_4N) (**4b**)	0.09	−0.11	1	30
[Fe]C≡C(C_6H_4)Br (**3d**)	0.08	−0.12	1	this work
[Fe]C≡C(C_6H_4)F (**3e**)	0.08	−0.15	1	this work
[Fe]C≡C(C_6H_5) (**3f**)	0.08	−0.15[b]	1	24
[Fe]C≡C(C_6H_4)CH_3 (**3g**)	0.08	−0.18	1	this work
[Fe]C≡C(C_6H_4)^{t}Bu (**3h**)	0.08	−0.18	1	this work
[Fe]C≡C(C_6H_4)OMe (**3i**)	0.15	−0.21	1	this work
[Fe]C≡C(C_6H_4)NH_2 (**3j**)	0.08	−0.25	1	this work
	0.17	+0.68	0.6	
[Fe]C≡C(C_6H_4)NMe_2 (**3k**)	0.09	−0.28	1	this work
	0.11	+0.53	0.6	

[a] All E values in V vs SCE. Conditions: CH_2Cl_2 solvent, 0.1 M [n-Bu_4N^+][PF_6^-] supporting electrolyte, 20 °C, Pt electrode, sweep rate 0.100 V s^{-1}. The ferrocene/ferrocenium (Fc/Fc^+) was used as an internal reference for potential measurements.[76] [b] E_0 values corrected for Fc/Fc^+ at 0.460 V vs SCE in CH_2Cl_2.

methyl protons of the cyclopentadienyl ligand, and there is apparently a gross correlation between the respective shifts of these signals (see the Supporting Information).

The complexes are also characterized by a strong infrared absorption at 2000−2060 cm^{-1}, which corresponds to the C≡C stretching mode. For the Fe(II) acetylides, very similar spectra were recorded in Nujol mulls (see the Experimental Section) and in solution (Table 1). In some cases, such as for **3a**,**b**, two absorptions are observed, while only one would be expected for the single triple bond in such a complex. The same splitting is possibly also present in **3c**, but in this case the second absorption shows up as a shoulder on the main one. Such a splitting of the $\nu_{C\equiv C}$ absorption is not attributable to packing effects, since it is observed in solution as well.[33] The presence of conformers (rotamers) is also unlikely, since the energetic barrier for rotation around the single bond appears negligible.[1] Thus, the only remaining explanation is to consider Fermi resonance.[34] It was established in many instances that acetylenic vibrations could exhibit Fermi coupling, provided an overtone vibrational band of neighboring atoms has exactly the same frequency as the C≡C vibrator.[35−39]

The cyclic voltammograms (CV) of all complexes display a reversible one-electron wave (Table 2) in the range +0.02/−0.28 V vs the standard calomel electrode (SCE) and a second irreversible process located in the solvent edge between 1.35 and 1.40 V. The reversible process corresponds to the well-known metal-centered Fe(II)/Fe(III) oxidation, and as expected, it indicates that the Fe(III) analogues are stable at the electrode.[18] It is immediately apparent that an electron-releasing substituent makes the oxidation of the iron(II) center easier. Similar qualitative trends for substituent effects have often been reported with other acetylide complexes.[32,40,41] The irreversible process involves apparently more than one electron and results possibly from the chemical decomposition of the corresponding Fe(IV) species at the Pt electrode.[42] In addition to these common processes, a third redox event can be observed for **3a**,**j**,**k**. Indeed, for complex **3a**, an additional reversible wave is present around very cathodic potentials (−1.28 V). This process corresponds to the one-electron reduction of the nitroaryl group in **3a** and is detected at −1.19 V for nitrobenzene and −1.01 V for (*p*-nitrophenyl)(trimethylsilyl)acetylene under similar conditions. The relative cathodic shifts of, respectively, 0.09 and 0.27 V observed for complex **3a** illustrate the electrodonating power of the iron(II) center, rendering the reduction of the nitroaryl ligand more difficult. For complexes **3j**,**k**, an additional quasi-reversible process is observed, respectively. around 0.7 and 0.5 V, which this time corresponds to the oxidation of the appended amino group. Expectedly, this process is easier (0.16 eV) for **3k** than for **3j**. Similar oxidations can be detected with aniline or *N*,*N*′-diethylaniline at, respectively, 1.19 and 0.90 V, and the cathodic shift observed for the complexes **3i**,**j** arises from the (still) electron-donating nature of the 17e fragment [(η^2-dppe)(η^5-C_5Me_5)Fe^{III}]$^+$.

Scheme 3

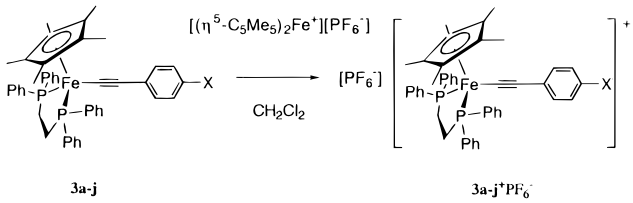

Synthesis and Characterization of the Oxidized Complexes. As suggested by the cyclic voltamogramms, the oxidized parents of **3a**−**k** are thermally stable at room temperature.[24] Accordingly, we have generated the hexafluorophosphate salts of the corresponding radical cations [(η^2-dppe)(η^5-C_5Me_5)FeC≡C(C_6H_4)X]$^{\bullet+}$ by chemical oxidation of their neutral parents (**3a**−**k**) using [(η^5-C_5H_5)$_2Fe^+$][PF_6^-] and characterized these compounds in situ by IR spectroscopy (Scheme 3). The complexes were also isolated in the two extreme cases, i.e., with the strongly electron-withdrawing nitro substituent (**3a**$^+$-PF_6^-) and with the strongly electron-releasing amino substituent (**3j**$^+PF_6^-$), while (**3f**$^+PF_6^-$) was already known.[24] Characterization of **3a**$^+PF_6^-$ and **3j**$^+PF_6^-$ was performed by the usual spectroscopic methods comple-

(32) (a) Younus, M.; Long, N. J.; Raithby, P. R.; Lewis, J.; Page, N. A.; White, A. J. P.; Williams, D. J.; Colbert, M. C. B.; Hodge, A. J.; Khan, M. S.; Parker, D. G. *J. Organomet. Chem.* **1999**, *578*, 198−209. (b) Touchard, D.; Haquette, P.; Daridor, A.; Romero, A.; Dixneuf, P. H. *Organometallics* **1998**, *17*, 3844−3852.

(33) Crystalline samples of **3a**,**b** gave exactly the same spectra as powderish samples, both in Nujol mulls and CH_2Cl_2 solutions.

(34) Silverstein, R. M.; Morrill, T. C.; Bassler, G. C. *Spectrometric Identification of Organic Compounds*; Wiley: New York, 1991.

(35) Without occurrence of Fermi coupling, harmonic or overtone bands are normally much less intense than any of the observed absorptions.[34]

(36) Fontaine, M.; Chauvelier, J.; Barchewitz, P. *Bull. Chim. Soc. Fr.* **1962**, 2145−2150.

(37) Queniec, R.; Wojtkowiak, B. *C. R. Acad. Sci. Paris* **1966**, *262*, 486−488.

(38) Grindley, T. B.; Johnson, K. F.; Katritzky, A. R.; Keogh, H. J.; Thirkettle, C.; Topsom, R. D. *J. Chem. Soc., Perkin Trans. 2* **1974**, 282−289.

(39) Markwell, R. D.; Butler, I. S.; Kakkar, A. K.; Khan, M. S.; Al-Zahkawani, Z. H.; Lewis, J. *Organometallics* **1996**, *15*, 2331−2337.

(40) For instance, a 0.2 V shift to higher oxidation potential is reported in the related Ru series for the *p*-nitrophenyl analogue relative to the unsubstituted complex.[41]

(41) Whittall, I. R.; Humphrey, M. G.; Hockless, D. C. R.; Skelton, B. W.; White, A. H. *Organometallics* **1995**, *14*, 3970−3979.

(42) Tilset, M.; Hamon, J.-R.; Hamon, P. *Chem. Commun.* **1998**, 765−766.

Downloaded by NORTH CAROLINA CONSORTIUM on June 29, 2009
Published on September 9, 2000 on http://pubs.acs.org | doi: 10.1021/om000325o

Table 3. ^{57}Fe Mössbauer Fitting Parameters at 80 K for Selected Complexes

compd	δ (mm s^{-1})	ΔE_Q (mm s^{-1})	Γ (mm s^{-1})	% area	ref
3a	0.256	2.061	0.114	100	this work
3a[a]	0.182	2.050	0.115	100	this work
3a$^+$PF$_6^-$	0.120	0.870	0.157	100	this work
3f[b]	0.28	2.02	n.r.[c]	100	24
3f$^+$PF$_6^-$[b]	0.25	0.90	n.r.[c]	100	24
3j	0.282	2.046	0.121	100	this work
3j$^+$PF$_6^-$	0.218	0.846	0.140	100	this work

[a] Value recorded at 293 K. [b] Value recorded at 77 K. [c] Not reported.

mented by elemental analysis. For **3j**$^+$PF$_6^-$, the possible presence of pentane as a solvate precluded obtaining a correct analysis. As expected, these dark compounds present a voltammogram identical with those obtained for their neutral parents **3a**,**j**, while their spectroscopic characteristics resemble these reported for **3f**$^+$PF$_6^-$[24] or other oxidized iron(III) alkynyls such as **4a**−**c**$^+$PF$_6^-$.[30]

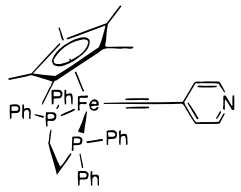

4a

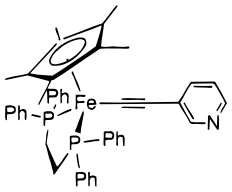

4b

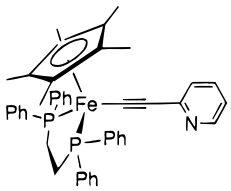

4c

The complexes isolated under two redox states (**3a**/**3a**$^+$PF$_6^-$) and (**3j**/**3j**$^+$PF$_6^-$) were also characterized by Mössbauer spectroscopy at 80 K. The results are reported in Table 3 and compared to measurements already found for **3f** and **3f**$^+$PF$_6^-$.[24] The present isomeric shift (IS) and quadrupolar splitting (QS) values for all neutral complexes are respectively very close together. This is also the case for all cationic complexes taken together and is evidence that **3a**,**j** and **3a**$^+$PF$_6^-$, **3j**$^+$PF$_6^-$ are respectively typical iron(II) and iron(III) alkynyls.[43] EPR spectroscopy of **3a**$^+$PF$_6$ and **3j**$^+$PF$_6^-$ confirms that these are stable metal-centered radicals in solution as well.[1,18]

IR characterization of the complexes was effected in CH_2Cl_2, after in situ oxidation from the neutral parents **3a**−**k** in the cell (Table 1). We have verified that neither the [(η^5-C_5H_5)$_2$Fe$^+$][PF$_6^-$] oxidant nor the generated (η^5-C_5H_5)$_2$Fe presented any absorptions in the spectral region of interest. Worthy of note is the fact that the IR spectra recorded in the 2500−1600 cm^{-1} range by this means, from **3a**,**f**,**j**, were rigorously identical with the spectra recorded from the isolated complexes **3a**$^+$PF$_6^-$, **3f**$^+$PF$_6^-$, and **3j**$^+$PF$_6^-$ in CH_2Cl_2. In the case of **3d**$^+$PF$_6^-$, **3f**$^+$PF$_6^-$, and **3j**$^+$PF$_6^-$ a splitting is observed in solution and also in the solid state for **3f**$^+$PF$_6^-$ (2025 and 1993 cm^{-1} in Nujol) and **3j**$^+$PF$_6^-$ (1988 and 1962 cm^{-1} in Nujol). As was the case with the neutral parents, this can be attributed to Fermi coupling. For **3d**$^+$PF$_6^-$−**3k**$^+$-PF$_6^-$, the absorption corresponding to the $\nu_{C\equiv C}$ stretch is shifted to lower wavenumbers relative to the respective neutral parents ($\Delta\nu_{C\equiv C}$). The shift is particularly pronounced (ca. 98 cm^{-1}) with complexes presenting electron-donating groups appended to the phenyl ring. On the other hand, for the compound **3a**$^+$PF$_6^-$, a 16 cm^{-1} shift in the opposite direction relative to the center of the Fermi doublet (2022 cm^{-1}) is stated, while in the case of the complexes **3b**$^+$PF$_6^-$ and **3c**$^+$PF$_6^-$, the intensity corresponding to the $\nu_{C\equiv C}$ stretch is apparently too weak to be observed in solution. In these cases, it has been checked that in situ reduction of the observed species with cobaltocene did restore the original absorption pattern of the neutral complexes **3b**,**c**, respectively. Additionally, for **3b**$^+$PF$_6^-$, the oxidation is evidenced by a 11 cm^{-1} shift of the C≡N stretching mode toward higher wavenumbers, due to the decreased retrodonation of the aryl ring in the antibonding π*(C≡N) orbitals. This slight strengthening of the C≡N bond results from the decreased π-electron richness of the aryl ring provoked by oxidation of its appended organometallic [(η^2-dppe)(η^5-C_5Me_5)Fe(C≡C)] substituent.

X-ray Structures of 3a,b, 3f·C$_5$H$_{12}$, and 3a$^+$PF$_6^-$·C$_4$H$_{10}$O. Monocrystals of **3a**,**b**,**f** and **3a**$^+$PF$_6^-$ could be grown, and the corresponding solid-state structures could be solved (Figures 1−4). The X-ray data are listed in Table 4, while the relevant bond angles and distances are given in Table 5.

The substituted neutral complexes **3a**,**b** crystallize in the same space group, which is different from that for the unsubstituted **3f**·C_5H_{12}. On the whole, the bond distances and angles are typical for piano-stool σ-organoiron(II) complexes (Figures 1−3).[18] Nevertheless, slight perturbations of the phenylalkynyl ligand are induced by the electroattracting substituents in **3a**,**b**. First, the triple bond presents a very small elongation (0.009 and 0.011 Å, respectively) relative to **3f**·C_5H_{12}. The latter has a bond-length value typical for such a phenylalkynyl complex (1.210 Å).[7] Also, the Fe−C37 bond is shorter in **3a**,**b** than in **3f**·C_5H_{12}. Albeit small, this shortening is more significant (0.018 and 0.015 Å, respectively). Complexes **3a**,**b** present the shortest values reported to date for such (η^2-dppe)(η^5-C_5Me_5)Fe^{II} fragments in neutral σ-alkynyl complexes of iron(II).[7] Additionally, the distance C38−C39 is also shorter for **3a** than for **3f**·C_5H_{12}, which also presents the normal value for such a bond (1.434 Å). In comparison to **3f**·C_5H_{12}, the aryl ring exhibits a very slight quinoidal-like departure from symmetry. In **3a**, the structural features of the nitro group are indicative of conjugation with the ring as well: (i) coplanarity of the aryl and nitro fragments (dihedral angle of 8.3(7)°) and (ii) a shorter C42−N1 bond relative to its expected mean value (1.455 vs 1.468 Å).[44,45] In **3b**, relative to **3f**·C_5H_{12}, small deformations comparable to these present in **3a** also take place for the phenylethynyl fragment. In this

Downloaded by NORTH CAROLINA CONSORTIUM on June 29, 2009
Published on September 9, 2000 on http://pubs.acs.org | doi: 10.1021/om000325o

(43) Guillaume, V.; Thominot, P.; Coat, F.; Mari, A.; Lapinte, C. *J. Organomet. Chem.* **1998**, *565*, 75−80.

(44) Allen, F. H.; Kennard, O.; Watson, D. G.; Brammer, L.; Orpen, A. G.; Taylor, R. *J. Chem. Soc., Perkin Trans. 2* **1987**, S1−S19.

Table 4. Crystal Data, Data Collection, and Refinement Parameters for 3f·C_5H_{12}, 3a,b, and 3a$^+PF_6^-$·$C_4H_{10}O$

	3f·C_5H_{12}	**3a**	**3b**	**3a**$^+PF_6^-$·$C_4H_{10}O$
formula	$C_{44}H_{44}P_2Fe·C_5H_{12}$	$C_{44}H_{43}NO_2P_2Fe$	$C_{45}H_{43}NP_2Fe$	$C_{44}H_{43}NO_2P_2FePF_6·C_4H_{10}O$
fw	762.73	735.58	715.59	954.67
temp (K)	293	293(2)	293	293(2)
cryst syst	monoclinic	triclinic	triclinic	monoclinic
space group	$P2_1/n$	$P\bar{1}$	$P\bar{1}$	$P2_1/n$
a (Å)	13.806(2)	12.131(3)	12.056(7)	15.444(2)
b (Å)	22.282(2)	12.190(3)	12.287(2)	16.606(4)
c (Å)	14.392(1)	15.223(2)	15.388(3)	16.807(3)
α (deg)	90.00	95.110(2)	73.33(1)	90.00
β (deg)	107.31(1)	105.910(2)	71.61(2)	94.290(10)
γ (deg)	90.00	116.590(3)	60.63(3)	90.00
V (Å^{-3})	4226(1)	1876.3(7)	1861(1)	4298.3(14)
Z	4	2	2	4
D_{calcd} (g cm^{-3})	1.199	1.302	1.277	1.475
cryst size (mm)	0.22 × 0.20 × 0.15	0.45 × 0.35 × 0.35	0.35 × 0.26 × 0.12	0.38 × 0.35 × 0.30
F(000)	1624	772	752	1988
diffractometer	CAD4	CAD4	CAD4	CAD4
radiation	Mo Kα	Mo Kα	Mo Kα	Mo Kα
abs coeff (mm^{-1})	0.465	0.525	0.524	0.533
θ range (deg)	2−27	1.44−24.97	1.41−26.97	1.73−26.97
hkl range	0−15, 0−28, −18 to +17	0−13, −14 to +12, −18 to +17	0−12, −13 to +15, −18 to +19	0−18, 0−21, −21 to +21
total no. of rflns	9205	6873	8081	9563
no. of unique rflns	8827	6533	7686	9216
no. of obsd rflns ($I > 2\sigma(I)$)	8827	4999	4149	5813
no. of restraints/params	0/453	0/452	0/443	0/537
a, b for w^a	0.0791, 0.5025	0.0600, 0.7368	0.1042, 0.0000	0.0981, 4.5546
final R	0.0530	0.0381	0.0658	0.0577
R_w	0.1287	0.0988	0.1602	0.1581
R (all data)	0.1271	0.0650	0.172	0.1177
R_w (all data)	0.1529	0.1080	0.1966	0.1854
goodness of fit/F^2	1.006	1.036	0.979	0.990
largest diff peak, hole (e Å^{-3})	0.507, −0.263	0.331, −0.307	1.133, −0.580	0.712, −0.657

[a] $w = 1/[\sigma^2(F_o^2 + (aP)^2 + bP]$, where $P = (F_o^2 + F_c^2)/3$.

respect, a remarkable common feature in the solid-state structures of **3a**,**b** is the unusual bending (C37−C38−C39 angles of, respectively, 173.5 and 173.8°) of the 4-substituted alkynylethynyl fragment. A typical value for such angles in alkynyl complexes is usually around 177°.[7] A close examination of the crystallographic cell suggests that this deformation may allow achieving a denser packing (see the Supporting Information).[46] Several researchers, to rationalize similar effects, recently invoked packing as well.[47−49]

Table 5. Selected Bond Lengths (Å) and Angles (deg) for or 3f·C_5H_{12}, 3a,b, and 3a$^+PF_6^-$·$C_4H_{10}O$

	3f·C_5H_{12}	**3a**	**3b**	**3a**$^+PF_6^-$·$C_4H_{10}O$
		Bond Distances		
Fe−$Cp_{centroid}$	1.740(4)	1.739(3)	1.739(5)	1.785(5)
Fe−P1	2.174(1)	2.1857(8)	2.1923(18)	2.2767(12)
Fe−P2	2.185(1)	2.1911(8)	2.1811(16)	2.2660(12)
Fe−C37	1.894(3)	1.876(3)	1.879(5)	1.892(4)
C37−C38	1.210(4)	1.220(4)	1.221(7)	1.215(5)
C38−C39	1.430(4)	1.419(4)	1.428(7)	1.437(5)
C39−C40	1.380(5)	1.401(4)	1.388(7)	1.384(6)
C40−C41	1.384(6)	1.374(4)	1.360(7)	1.380(6)
C41−C42	1.358(8)	1.368(4)	1.390(8)	1.362(7)
C42−C43	1.337(7)	1.368(4)	1.378(8)	1.360(7)
C43−C44	1.380(5)	1.373(4)	1.373(8)	1.383(6)
C44−C39	1.378(5)	1.394(4)	1.411(8)	1.385(6)
C42−C45			1.441(8)	
C45−N1			1.130(7)	
C42−N1		1.455(4)		1.468(6)
N1−O1		1.215(4)		1.215(8)
N1−O2		1.208(4)		1.206(8)
		Bond Angles		
P1−Fe−P2	85.92(4)	86.56(3)	82.42(6)	83.33(4)
P1−Fe−C37	87.0(1)	82.26(8)	87.24(15)	89.99(12)
P2−Fe−C37	83.9(1)	87.90(8)	82.49(16)	84.89(12)
Fe−C37−C38	176.6(3)	178.3(3)	178.6(2)	175.5(4)
C37−C38−C39	177.7(4)	173.5(3)	173.8(6)	176.6(5)
C40−C39−C44	116.8(3)	117.4(3)	116.6(5)	118.8(4)
C41−C42−C43	119.5(5)	121.9(3)	118.9(5)	122.4(4)
C41−C42−C45			120.3(6)	
C42−C45−N1			179.3(8)	
C42−N1−O1		118.6(3)	118.5(5)	117.6(6)
C42−N1−O2		118.8(3)	117.8(5)	118.6(6)
O1−N1−O2		122.6(3)	123.7(5)	123.7(6)

The oxidized **3a**$^+PF_6^-$·$C_4H_{10}O$ compound crystallizes in the monoclinic space group with a disordered PF_6^- anion. Relative to **3a**, weak structural modifications

(45) Analogous quinoid-like deformations of the phenylethynyl fragment take place in related Ru acetylides despite a different (perpendicular) orientation of the phenyl ring[41] and were imparted to conjugation of the nitro group with a strong donor in the *para* position.[85] For donor−acceptor polyynes similar deformations were reported as well. Interestingly in this case, as for **3a**, the C≡C bond lengths were barely affected, despite an obvious *intramolecular* charge-transfer character.[50]

(46) DFT calculations indicate that structure D (Scheme 4) for **3a** is comparable in stability (ca. ±0.001 eV) to B (Scheme 4).[1] The observed bending could thus be envisioned as resulting from a weight of ca. 12% of D, where pseudo-H bonding would stabilize the electronic density on the β-carbon. Accordingly, in **3a**,**b** the closest contacts with the respective β-carbon atoms are achieved in an intramolecular fashion with a hydrogen atom (the C−H distance is 2.80/3.58 Å for C38−C8 in **3a**, and the C−H distance is 2.79/3.56 Å for C38−C9 in **3b**) of a η^5-C_5Me_5 methyl group. Although these hydrogen atoms were not observed but set in place, their eclipsed position results from an *R*-minimization process allowing free rotation of the methyl group. We do not, however, favor this "intramolecular" explanation, since the α-carbon in both complexes is even closer from this hydrogen (C−H distance of 2.61/3.13 Å for C37−C8 in **3a** and C−H distance of 2.62/3.13 Å for C37−C9 in **3b**), and this makes sense with regard to the observed bending.

(47) Whittall, I. R.; Cifuentes, M. P.; Humphrey, M. G.; Luther-Davies, B.; Samoc, M.; Houbrechts, S.; Persoons, A.; Heat, G. A.; Hockless, D. C. R. *J. Organomet. Chem.* **1997**, *549*, 127−137.

(48) Dembinski, R.; Lis, T.; Szafert, S.; Magne, C. L.; Bartik, T.; Gladysz, J. A. *J. Organomet. Chem.* **1999**, *578*, 229−246.

(49) Peters, T. B.; Bohling, J. C.; Arif, A. M.; Gladysz, J. A. *Organometallics* **1999**, *18*, 3261−3263.

Downloaded by NORTH CAROLINA CONSORTIUM on June 29, 2009
Published on September 9, 2000 on http://pubs.acs.org | doi: 10.1021/om000325o

Table 6. UV−Vis Data for Selected Complexes in CH_2Cl_2

compd	λ, nm ($10^{-3}\epsilon$, M^{-1} cm^{-1})	ref
[Fe]C≡C(C_6H_4)NO_2 (**3a**)	258 (sh, 21.1); 334 (11.6); 595 (13.0)	this work
[Fe]C≡C-*p*-(C_6H_4N) (**4a**)	260 (sh, 23.2); 403 (7.9)	26
[Fe]C≡C(C_6H_4)CN (**3b**)	267 (sh, 17.8); 281 (sh, 16.1); 387 (sh, 10.3); 445 (16.4)	this work
[Fe]C≡C(C_6H_4)CF_3 (**3c**)	258 (sh, 30.6); 387 (13.2)	this work
[Fe]C≡C−o-(C_6H_4N) (**4c**)	265 (sh, 23.6); 374 (9.0); 391 (sh, 8.9)	26
[Fe]C≡C-*m*-(C_6H_4N) (**4b**)	265 (sh, 25.4); 363 (10.7); 401 (sh, 8.3)	26
[Fe]C≡C(C_6H_4)Br (**3d**)	323 (sh, 16.4); 356 (13.8); 391 (sh, 11.2)	this work
[Fe]C≡C(C_6H_4)F (**3e**)	302 (sh, 11.8); 328 (sh, 9.9); 351 (sh, 9.0)	this work
[Fe]C≡C(C_6H_5) (**3f**)	277 (sh, 14.5); 350 (13.6)	this work
[Fe]C≡C(C_6H_4)CH_3 (**3g**)	283 (sh, 15.6); 301 (sh, 12.6); 339 (10.6)	this work
[Fe]C≡C(C_6H_4)^{t}Bu (**3h**)	255 (sh, 35.7); 282 (sh, 15.5); 343 (14.8)	this work
[Fe]C≡C(C_6H_4)OMe (**3i**)	282 (sh, 16.3); 333 (13.2)	this work
[Fe]C≡C(C_6H_4)NH_2 (**3j**)	252 (sh, 37.0); 282 (sh, 20.7); 322 (17.6)	this work

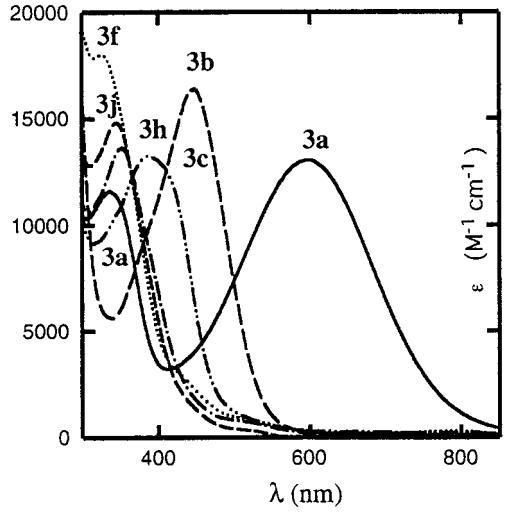

Figure 5. Selected UV−vis spectra of complexes in dichloromethane at 20 °C.

take place in **3a**$^+PF_6^-\cdot C_4H_{10}O$, both in the coordination sphere of the metal and in the arylethynyl fragment (Table 4).[18] The Fe−P distances as well as the Fe−(η^5-C_5Me_5) centroid are elongated with a concomitant shortening of the P−aryl bonds (ca. 0.08 Å), consistent with a decreased back-donation from the metal to antibonding orbitals in these ligands.[51] The Fe−C37 bond is slightly elongated upon oxidation (0.016 Å), but the phenyl core recovers a more regular structure with angles and distances resembling those reported for the neutral **3f**$\cdot C_5H_{10}$. The nitro group is still coplanar with the aryl group (dihedral angle of 5.8(5)°), but its bond distances are in the conventional range for such a substituent appended to an aryl group.[44]

UV−Vis Spectra of the Neutral Complexes. Except for **3k**, the UV−vis spectra were recorded for all complexes in the 250−900 nm range. These resemble the spectra previously reported for the related 4-pyridylethynyl organoiron(II) compounds **4a**.[26,30] Notably, for the neutral complexes (Figure 5 and Table 6), apart from the energetic transitions above 270 nm, which can safely be attributed to $\pi-\pi^*$ ligand-centered transitions, one broader and less intense transition is always present at higher wavelengths. This absorption is at the origin of the orange color of **3b**−**j** and also of the unusual purple color of the complex **3a**. This transition was previously attributed to a MLCT transition.[30] Accordingly, it is not observed in the spectra of the oxidized **3a**$^+PF_6^-$, **3j**$^+PF_6^-$, and **3f**$^+PF_6^-$ complexes, which, as mentioned previously, also resemble those reported for the oxidized analogues of the pyridylalkynyl complexes **4a**−**c**.[1,30] The MLCT transition in **3a**−**j** shifts toward lower energy with the increasing electron-withdrawing power of the appended substituent. In the case of the nitro-substituted complex (**3a**), a second transition of comparable intensity is present at 334 nm.[52] As for the former one at 595 nm, we attribute it to a MLCT transition, rather than to an n → p nitroaryl-centered transition. Such a transition appears usually at lower wavenumbers in nitrobenzene (350 nm) and is much less intense (ϵ = 200).[53]

Discussion

The influence of the substituent on the electronic properties in these Fe(II) and Fe(III) iron acetylides is shown by characteristic changes in the spectroscopic data gathered for **3a**−**k** and **3a**$^+PF_6^-$−**3k**$^+PF_6^-$. Notably, the effect on the alkynyl linker is apparent in the IR stretching frequency shifts relative to the unsubstituted complexes **3f**/**3f**$^+PF_6^-$.[54] The limited range of these indicates, however, that the triple-bond character is dominant in all compounds. More interestingly, oxidation provokes an opposite shift of the $\nu_{C\equiv C}$ signal, depending on the substituent present on the aryl group (Table 1; $\Delta\nu_{C\equiv C}$).

When the IR shifts are analyzed from the standpoint of π-interactions only (Scheme 4),[55] the lowering of the C≡C stretching frequency may be rationalized by considering an increased weight of cumulene-like mesomers (A/A′, C/C′, and D/D′) in the bonding description,[56] relative to the pure alkynyl structures (B/B′).[57−59] For Fe(II) acetylides, the wavenumbers corresponding

(50) Graham, E. M.; Miskowski, V. M.; Perry, J. W.; Coulter, D. R.; Stiegman, A. E.; Schaefer, W. P.; Marsh, R. E. *J. Am. Chem. Soc.* **1989**, *111*, 8771−8779.

(51) Orpen, A. G.; Connelly, N. G. *Organometallics* **1990**, *9*, 1206−1210.

(52) Both bands exhibit a weak solvatochromy ($\Delta\nu_{max}$[low-energy MLCT] = −46 nm in toluene and $\Delta\nu_{max}$[high-energy MLCT] = −15 nm in MeOH).

(53) Wheland, G. W. *Resonance in Organic Chemistry*; Wiley: New York, 1955; p 288.

(54) The pitfalls concerning the evaluation of π-bonding in alkynyl complexes using infrared spectroscopy have been underlined by many authors.[7,86] Such problems are, however, limited when comparison is made within a set of structurally similar complexes, as in the present case. The substituents being remote from the triple bond, substituent-specific undesirable mass effects or vibronic coupling should not infer with their purely electronic influence. For other related references, see refs 38, 68, 69, 71, and 87.

(55) The triple-bond stretch of a given metal alkynyl might also be influenced by the polarity of the M−C_α bond.[7] See also ref 88.

Downloaded by NORTH CAROLINA CONSORTIUM on June 29, 2009
Published on September 9, 2000 on http://pubs.acs.org | doi: 10.1021/om000325o

Scheme 4

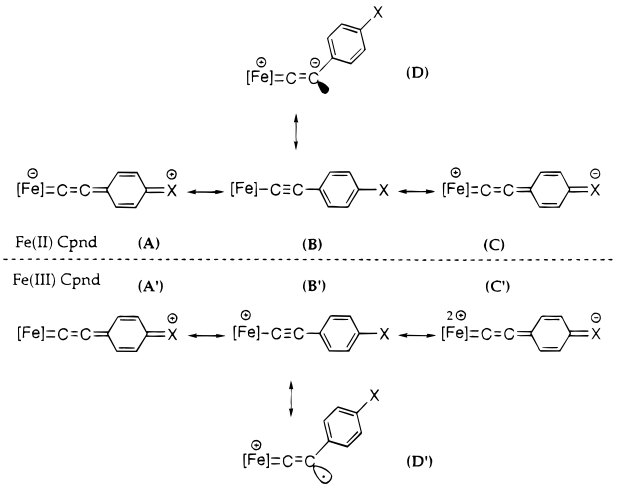

to the $\nu_{C\equiv C}$ stretch are roughly constant for most substituents (**3d**−**j**), except for the more electron-withdrawing ones (**3a**−**c**), where the alkynyl bond order appears slightly depressed (Table 1). The usual resonance rules suggest that this can reasonably result only from an increased weight of C or D.[60] Indeed, A would correspond to a very unstable 20e iron center and must be strongly disfavored relative to C and D, which present formally 18e metal centers. The effect of the substituent is different for the oxidized parents **3a**$^+$-PF_6^-−**3k**$^+PF_6^-$, where the bond order diminishes concomitantly with the increasing electron-donating power of the substituent. In this case, structures A′ and D′ may now constitute the most likely cumulenic contributors to the bonding scheme (respectively 19e and 18e iron centers), since C′ presents an unfavorable zwitterionic structure. The reversed shift noted for **3a** upon oxidation relative to **3d**−**j** can then be understood as resulting from a different balance between the classic alkynyl structures (B/B′) and oppositely polarized cumulene-like mesomers (C and D vs A′ and D′) in the Fe(II) and Fe(III) acetylides (Scheme 5). It constitutes an interesting experimental illustration of the strong synergy that can take place between the remote *para* substituent on the aryl ring and the iron center, depending on the oxidation state of the metal.

A close examination of our X-ray data was next achieved to complement these observations. On the whole, the structural changes observed for the Fe(II) acetylides, albeit weak, are exactly what would be expected if the limiting structure C (Scheme 4) would present an increased weight in the bonding description of **3a** relative to **3f**·C_5H_{12}.[45] Obviously, to evaluate the weight of a mesomer such as C in the Fe(II) acetylides, the shortening of the M−C_α distance[61,62] constitutes a far better test than the length of the C≡C bond itself.[63] In **3a,b** and **3f**·C_5H_{10} all Fe−C37 bond lengths (Table 4) are shorter than a typical Fe−C(sp^3) bond (2.003(4) Å in [(η^2-dppe)(η^5-C_5Me_5)$FeCH_2(OMe)^+$][PF_6^-]).[64] However, part of that shortening originates from the change in electronegativity of the sp-hybridized α-carbon. As thoroughly discussed by Hopkins et al.,[7] evaluation of this "normal" contribution to the shortening is possible when the group electronegativity of the metal fragment is known precisely. We could spectroscopically derive[65] an estimate of such a group electronegativity for the (η^2-dppe)(η^5-C_5Me_5)Fe fragment as being ca. 1.1.[66] We have next computed the theoretical distance-shortening contribution due to change in hybridization[67] amounting to 0.096 Å. The Fe−C_α bond shortening of 0.109 Å stated for **3f**·C_5H_{10} is typically in this range. However, considering that the electronegativity of the α-carbon will not change significantly in **3a**,**b**, the additional shortening of 0.018 or 0.015 Å observed may now be ascribed to M−C_α π-interactions (structure C; Scheme 4).

The structural changes between **3a** and **3a**$^+PF_6^-$·$C_4H_{10}O$ were also carefully compared, since very few solid-state structures are available for the same transition-metal acetylide under two different redox states.[68,69] While the oxidation state of the metal center is apparently not a determining factor affecting the Fe−C37 (and also C37−C38) bond length in **3a** and **3a**$^+PF_6^-$·$C_4H_{10}O$ (Table 4), the slight distortion of the aromatic ring possibly has such an origin. This would be consistent with the picture deduced from IR data regarding the Fe−C_α and C≡C bond orders. Accordingly, the magnitude of the structural changes also suggests that the weight of the cumulene-like mesomers in **3a** must be very small in the solid state. This is also evidenced by Mössbauer spectroscopy, which constitutes an alternative means to detect significant π-bonding changes

(56) Structures such as A/A′ and C/C′ are classic mesomeric contributors usually envisioned for organic and organometallic acetylides,[89] while D, and to a greater extent D′, may take part in the reactivity of related iron acetylides.[21,30] Both A/A′ and C/C′ imply a relative loss of aromaticity relative to B/B′, whereas D/D′ require a geometric deformation of the acetylide−aryl fragment and are in fact limiting cases between tautomers (although no bond is broken relative to B/B′) and true mesomers.[46]

(57) Eiduss, J.; Korshunov, S. P.; Vereshagin, L. I.; Venters, K.; Hillers, S. In *Chemistry of Acetylene, Transactions of the All-Union Conference on the Chemistry and Technology of Acetylene*; Petrov, A. A., Ed.; Izd. "Nauka": Moscow, 1968; pp 411−414; *Chem. Abstr.* **1969**, *70*, 110255q.

(58) Zeil, W.; Haase, J.; Dakkouri, M. *Discuss. Faraday. Soc.* **1969**, *47*, 149−156.

(59) Buchert, H.; Zeil, W. *Spectrochim. Acta* **1962**, *18*, 1043−1053.

(60) March, J. *Advanced Organic Chemistry: Reactions, Mechanisms and Structure*, 4th ed.; Wiley: New York, 1992.

(61) Spofford, W. A., III; Carfagna, P. D.; Amma, E. L. *Inorg. Chem.* **1967**, *6*, 1553−1557.

(62) Nast, R.; Beyer, A. *J. Organomet. Chem.* **1981**, *204*, 267−272.

(63) The constancy of bond lengths in (poly)ethynyl fragments has often been reported, and distortions were usually rationalized by packing effects.[7,86,91] Spectroscopic data also suggest that the length of the acetylenic bond is rather insensitive to substitution or changes in polarization.[58,92] Moreover, the acetylenic carbon atoms often present large anisotropies, which limits precise appreciation of bond lengths, and it has been proposed that the RX data for the C≡C bond length should be considered only when determined with at least 0.010 Å accuracy.[7] This the case for all structures reported here.

(64) Roger, C.; Toupet, L.; Lapinte, C. *J. Chem. Soc., Chem. Commun.* **1988**, 713−715.

(65) We have used the empirical $\nu_{C\equiv C}$ vs electronegativity correlation (1) established for the PhC≡CX series by Wojtkowiak et al. from the $\nu_{C\equiv C}$ value measured for **3f**·C_5H_{10} in Nujol mull (2048 cm^{-1}).[88]

$$\nu_{PhC\equiv CX}\ (cm^{-1}) = 159\chi_X + 1875 \qquad (1)$$

(66) Expectedly, this value is inferior to the group electronegativity of 2.27 estimated for the (η^5-C_5H_5)$Fe(CO)_2$ fragment.[84]

(67) We have used eq 2, reported by Hopkins et al. and derived from the Schomaker−Stevenson equation, with $r_{C(sp^3)} = 2.48$ (Pauling) and $r_{C(sp)} = 2.56$ (group electronegativity for "−C≡CPh").[7]

$$D(M{-}C) = 0.08{-}0.07(X_{Fe} - X_{C(sp^3)})^2 + 0.07(X_{Fe} - X_{C(sp)})^2 \qquad (2)$$

(68) Bianchini, C.; Laschi, F.; Masi, D.; Ottaviani, F. M.; Pastor, A.; Peruzzini, M.; Zanello, P.; Zanobini, F. *J. Am. Chem. Soc.* **1993**, *115*, 2723−2730.

(69) Beddoes, R. L.; Bitcon, C.; Whiteley, M. W. *J. Organomet. Chem.* **1991**, *402*, 85−96.

Downloaded by NORTH CAROLINA CONSORTIUM on June 29, 2009
Published on September 9, 2000 on http://pubs.acs.org | doi: 10.1021/om000325o

Scheme 5

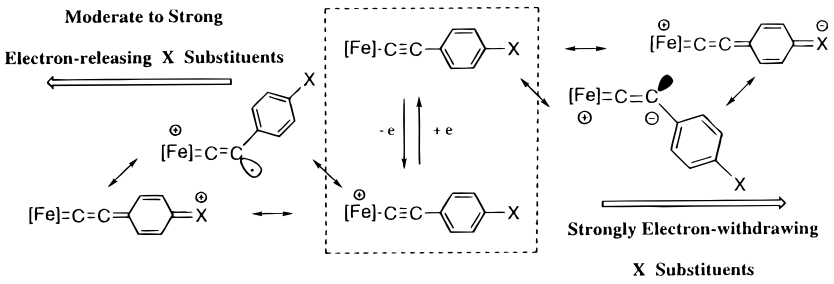

Table 7. Selected Bond Lengths (Å) Already Reported for Structurally Characterized Redox Congeners among Transition-Metal Acetylides

compd	M−P	M−C	C≡C	Δ(M−C)	ref
7[a]	2.467(1)	2.138(5)	1.205(6)		69
	2.477(1)				
7$^+BF_4^-$[b]	2.538(2)	2.067(9)	1.196(11)	0.071(14)	69
	2.528(3)				
8[c]	2.214(3)	1.92(1)	1.21(1)		68
	2.212(3)				
	2.187(3)				
	2.153(3)				
8$^+BPh_4^-$·THF[d]	2.315(6)	1.88(2)	1.20(3)	0.04(3)	68
	2.292(6)				
	2.301(6)				
	2.225(6)				

[a] $R = 0.0433$, $R_w = 0.0471$, $S = 0.959$. [b] $R = 0.0599$, $R_w = 0.0553$, $S = 0.970$. [c] $R = 0.061$, $R_w = 0.068$, S not reported. [d] $R = 0.079$, $R_w = 0.079$, S not reported.

in similar complexes.[43] Thus, considering the QS magnitude as an indicator of the "cumulenic" character of the alkyne linker, only insignificant changes are stated between the QS values found for **3a** and **3j** or **3a**$^+PF_6^-$ and **3j**$^+PF_6^-$ (Table 3).

In the literature, only a few studies have been conducted on redox congeners with mononuclear σ-alkynyl complexes, and these studies usually involved fewer compounds. The reported changes in the triple-bond stretching frequencies upon oxidation vary, depending on the compounds under investigation. A shift to lower wavenumbers (13 cm^{-1}) has been reported with the d^6 piano-stool complexes $\{(\eta^2\text{-dppe})(\eta^7\text{-}C_7H_7)Mo(C{\equiv}CPh)\}^{n+}(BF_4^-)_n$ ($n = 0$, 1; **7**/**7**$^+BF_4^-$) by Beddoes et al.,[69] while the opposite behavior was stated for d^7 trigonal-bipyramidal complexes such as $\{[\eta^4\text{-}P(CH_2CH_2PPh_2)_3]Co(C{\equiv}CR)\}^{n+}(BPh_4^-)_n$ and $\{[\eta^4\text{-}N(CH_2CH_2PPh_2)_3]Rh(C{\equiv}CR)\}^{n+}(BPh_4^-)_n$ ($n = 0$, 1; R = Ph, CO_2Et) studied by Bianchini et al.[70,71] A shift of 30−35 cm^{-1} was observed for both metal complexes and was taken as evidence for retrodonation, which would formally correspond to Lewis structures such as C and D in Scheme 4. The weakness of the IR shifts in σ-alkynyl complexes is in line with the global constancy of the structural features of the acetylide linker upon oxidation reported for the even fewer examples available (Table 7).[68,69] Interestingly, in the case of the Fe(I/II) trigonal-bipyramidal complexes $\{[\eta^4\text{-}P(CH_2CH_2PPh_2)_3]Fe(C{\equiv}C{-}C_6H_5)\}^{n+}(BPh_4^-)_n$ ($n = 0$, 1; **8**/**8**$^+BPh_4^-$), despite the very increased electronic richness of the metal center relative to **3a**−**k**, no marked change in the stretching frequency was noted between **8** and **8**$^+BPh_4^-$. This indicates that, in the lower oxidation state, not only the electronic density on the metal center but also the geometry and the nature of the metal center have a determining influence on the weight of limiting structures A and D.

As surmised at the beginning of this work, the present mononuclear Fe(II) and Fe(III) complexes appear to constitute promising models to study the intimate redox-dependent electronic changes taking place in related binuclear ethynylaryl complexes.[19,72,73] Currently, for most compounds of this type, a decrease in the triple-bond stretching frequency is always observed upon complete oxidation and attributed to limiting mesomeric structures somewhat resembling D′ and A′. The precise knowledge of the "cumulenic character" of the bridging unit in such complexes is very interesting, since such a character may determine the magnitude of the magnetic exchange coupling (J_{AB}) between the remote metal sites in the dioxidized state[74] but certainly also the magnitude of the electronic coupling parameter (V_{AB} or H_{AB}) in the mixed-valent state. Additionally, these mononuclear models may also provide precious bits of information in other regards. For instance, the closeness of the structural parameters between **3a** and **3a**$^+PF_6^-$·$C_4H_{10}O$ suggests that the oxidation of the iron center in $(\eta^2\text{-dppe})(\eta^5\text{-}C_5Me_5)Fe{-}C{\equiv}C$ fragments will be associated with a weak intramolecular reorganization energy (λ_{in}).[18,75]

In conclusion, we have reported here the synthesis of a family of substituted electron-rich Fe(II) and Fe(III) alkynyls and have characterized these compounds in two redox states. Both the influences of the redox state of the metal and the influence of the substituent on the electronic distribution in the alkynyl linker have been examined. While, as expected, the former effect overwhelms the second in most compounds, the IR data indicate nevertheless that the redox-induced changes can apparently be tuned or reversed, depending on the substituent present on the aryl group. This has been tentatively explained by a redox-dependent interplay of various cumulene-like mesomeric forms in addition to the dominant alkynyl structures B and B′. A consistent picture involving respectively C or D for the neutral

Downloaded by NORTH CAROLINA CONSORTIUM on June 29, 2009
Published on September 9, 2000 on http://pubs.acs.org | doi: 10.1021/om000325o

(70) Bianchini, C.; Meli, A.; Peruzzini, M.; Vacca, A.; Laschi, F.; Zanello, P.; Ottaviani, F. M. *Organometallics* **1990**, *9*, 360−371.
(71) Bianchini, C.; Innocenti, P.; Meli, A.; Perruzzini, M.; Zanobini, F.; Zanello, P. *Organometallics* **1990**, *9*, 2514−2522.
(72) Colbert, M. C. C.; Lewis, J.; Long, N. J.; Raithby, P. R.; Younus, M.; White, A. J. P.; Williams, D. J.; Payne, N. J.; Yellowlees, L.; Beljonne, D.; Chawdhury, N.; Friend, R. H. *Organometallics* **1998**, *17*, 3034−3043.
(73) Sato, M.; Shintate, H.; Kawata, Y.; Sekino, M.; Katada, M.; Kawata, S. *Organometallics* **1994**, *13*, 1956−1962.
(74) Paul, F.; Meyer, W.; Jiao, H.; Toupet, L.; Gladysz, J. A.; Lapinte, C. *J. Am. Chem. Soc.*, in press.
(75) A similar statement can be made for $(\eta^2\text{-dppe})(\eta^5\text{-}C_5Me_5)FeCl$ and $[(\eta^2\text{-dppe})(\eta^5\text{-}C_5Me_5)FeCl^+](PF_6^-)$, which constitute the only other set of redox congeners structurally characterized with the same metal fragment.[18]

compounds and A′ or D′ for the oxidized parents seems to emerge (Scheme 5). Obviously, **3a**−**k** and **3a**$^+PF_6^-$−**3k**$^+PF_6^-$ complexes constitute interesting mononuclear complexes that model the electronic changes induced by oxidation of the metal termini in related polynuclear phenylethynyl organometallic assemblies, and current work is in progress to obtain additional insight into the metal−bridge bonding in these complexes.[1]

Experimental Section

General Data. All manipulations were carried out under an inert atmosphere. Solvents or reagents were used as follows: Et_2O and *n*-pentane, distilled from Na/benzophenone; CH_2Cl_2, distilled from CaH_2 and purged with argon; $HN(^iPr)_2$, distilled from KOH and purged with argon; aryl bromides (Acros, >99%), opened/stored under Ar. HC≡C-1,4-(C_6H_4)-NH_2[29] and the complexes [(η^5-C_5H_5)$_2$Fe$^+$][PF_6^-],[76] (η^5-C_5Me_5)-Fe(η^2-dppe)(C≡CH) (**1**), and [(η^5-C_5Me_5)Fe(η^2-dppe)(C≡CPh)$^+$]-[PF_6^-] (**3f**$^+PF_6^-$) were prepared by previously published procedures.[24] High-field NMR experiments were performed on multinuclear Bruker 300 and 200 MHz instruments (AM300WB and 200DPX). Chemical shifts are given in parts per million relative to tetramethylsilane (TMS) for ^{1}H and ^{13}C NMR spectra and H_3PO_4 for ^{31}P NMR spectra. Transmittance-FTIR spectra were recorded using a Bruker IFS28 spectrometer (400−4000 cm^{-1}). UV−visible spectra were recorded on an UVIKON 942 spectrometer. Cyclic voltammograms were recorded using a PAR 263 instrument in CH_2Cl_2 (0.1 M (*n*-Bu)$_4$N$^+PF_6^-$) at 25 °C at a platinum electrode, using an SCE reference electrode and ferrocene as internal calibrant (0.460 V).[76] Mössbauer spectra were recorded with a 2.5 × 10^{-2} C (9.25 × 10^8 Bq) ^{57}Co source using a symmetric triangular sweep mode.[77] LSI-MS analyses were performed at the "Centre Regional de Mesures Physiques de l'Ouest" (Rennes, France; CRMPO) on a high-resolution MS/MS ZabSpec TOF Micromass spectrometer (8 kV). Elemental analyses were performed at the Centre for Microanalyses of the CNRS at Lyon-Solaise, France.

(η^2-dppe)(η^5-C_5Me_5)Fe[C≡C-1,4-(C_6H_4)NO_2] (3a). In a Schlenk tube, the orange complex **1** (0.200 g; 0.325 mmol), the (PPh_3)$_2$$PdCl_2$ catalyst precursor (0.023 g; 0.032 mmol), and CuI cocatalyst (0.013 g; 0.065 mmol) were introduced under argon. Subsequently *p*-bromonitrobenzene (0.120 g; 1.62 mmol) in 10 mL of diisopropylamine was added, and the mixture was heated at 60 °C for 12 h. The solvents were then cryogenically trapped, and the deep purple residue was extracted with toluene and filtered on a Celite pad. Evaporation of the toluene and washing with cooled acetonitrile (−20 °C, 5 mL) and *n*-pentane (−40 °C, 2 × 5 mL) yielded the desired complex (η^2-dppe)(η^5-C_5Me_5)Fe[C≡C-1,4-(C_6H_4)NO_2] (**3a**) as a purple solid (0.152 g; 0.208 mmol, 64%) after drying in vacuo. Crystals were grown by slow diffusion of *n*-pentane in a dichloromethane solution of **3a** (layer/layer). Anal. Calcd for $C_{44}H_{43}NO_2P_2Fe$: C, 71.84; H, 5.89; N, 1.90. Found: C, 71.56; H, 5.95; N, 1.99. MS (positive LSI, 3-NBA): *m*/*z* 735 ([**3a**,H]$^+$, 85%); 600 ([(dppe)FeC≡C(C_6H_4)NO_2]$^+$, 3%); 589 ([(dppe)(C_5Me_5)Fe]$^+$, 100%). FT-IR (ν, KBr/Nujol, cm^{-1}): 2038, 2005 (s, C≡C). ^{31}P NMR (δ, C_6D_6, 81 MHz): 100.6 (s, 2P, dppe). ^{1}H NMR (δ, C_6D_6, 200 MHz): 8.00 (d, 2H, $^3J_{HH}$ = 8.5 Hz, H_o($ArNO_2$)); 7.79 (m, 4H, H_o((Ar/dppe))); 7.35−7.00 (m, 16H, *H*(Ar/dppe)); 6.79 (d, 2H, $^3J_{HH}$ = 8.5 Hz, H_m($ArNO_2$)); 2.52 (m, 2H, CH_2(dppe)); 1.81 (m, 2H, CH_2(dppe)); 1.45 (s, 15H, C_5(CH_3)$_5$). ^{13}C{^{1}H} NMR (δ, C_6D_6, 50 MHz): 162.5 (t, $^2J_{CP}$ = 38 Hz, Fe−*C*≡C); 143.0 (s, C_{quat}-($ArNO_2$)); 139.1−127.7 (m, 8*C*(Ar/dppe) + *C*−H($ArNO_2$) + C_{quat}-($ArNO_2$)); 124.3 (m, *C*−H($ArNO_2$) and Fe−C≡*C*); 88.8 (s, C_5(CH_3)$_5$); 33.6−28.0 (m, CH_2(dppe)); 10.4 (s, $^1J_{CH}$ = 126 Hz, C_5(*C*H_3)$_5$).

(η^2-dppe)(η^5-C_5Me_5)Fe[C≡C-1,4-(C_6H_4)CN] (3b). The reaction was started as described for **3a** using 2.5 equiv of *p*-bromobenzonitrile (0.147 g; 0.812 mmol) instead of 5 equiv of nitrobenzene, but the reaction medium was now heated to reflux. In this case, the desired complex (η^2-dppe)(η^5-C_5Me_5)-Fe[C≡C-1,4-(C_6H_4)CN] (**3b**) is poorly soluble in diisopropylamine and most of it coprecipitates with the formed ammonium salt. Filtration of this precipitate followed by extraction with toluene (30 mL), reprecipitation with excess methanol, and subsequent methanol and *n*-pentane washings yielded **3b** as an orange solid (0.123 g; 0.171 mmol; 53%) after drying in vacuo. Crystals can be grown by slow diffusion of *n*-pentane in a dichloromethane solution of **3b** (layer/layer). Anal. Calcd for $C_{45}H_{43}NP_2Fe$: C, 75.53; H, 6.06; N, 1.96. Found: C, 75.39; H, 5.91; N, 2.02. MS (positive LSI, 3-NBA): *m*/*z* 716 ([**3b**,H]$^+$, 95%); 589 ([(dppe)(C_5Me_5)Fe]$^+$, 100%); 580 ([(dppe)Fe-C≡C(C_6H_4)CN]$^+$, 2%). FT-IR (ν, KBr/Nujol, cm^{-1}): 2017 (s, C≡N); 2047, 2028 (s, C≡C). ^{31}P NMR (δ, C_6D_6, 81 MHz): 100.9 (s, 2P, dppe). ^{1}H NMR (δ, C_6D_6, 200 MHz): 7.83 (m, 4H, H_o-(Ar/dppe)); 7.35−6.95 (m, 18H, *H*(Ar/dppe) + H_o(ArCN)); 6.82 (d, $^2J_{HH}$ = 8.4 Hz, 2H, H_m(ArCN)); 2.50 (m, 2H, CH_2(dppe)); 1.79 (m, 2H, CH_2(dppe)); 1.45 (s, 15H, C_5(CH_3)$_5$). ^{13}C{^{1}H} NMR (δ, $CDCl_3$, 50 MHz): 157.4 (t, $^2J_{CP}$ = 38 Hz, Fe-*C*≡C); 139.0−127.5 (m, 8*C*(Ar/dppe) + 2*C*−H(ArCN) + C_{quat}(ArCN)); 121.0 (s, Fe−C≡*C*); 119.5 (s, $^2J_{CH}$ = ca. 6 Hz, C_{quat}(ArCN)); 104.1 (s, $^3J_{CH}$ = 9 Hz, Ar−*C*N); 88.6 (s, C_5(CH_3)$_5$); 31.0 (m, CH_2(dppe)); 10.5 (s, $^1J_{CH}$ = 126 Hz, C_5(*C*H_3)$_5$).

(η^2-dppe)(η^5-C_5Me_5)Fe[C≡C-1,4-(C_6H_4)CF_3] (3c). The reaction was effected as described for **3b** with 2 equiv of *p*-(trifluoromethyl)bromobenzene (0.240 mL; 0.650 mmol). The desired complex (η^2-dppe)(η^5-C_5Me_5)Fe[C≡C-1,4-(C_6H_4)CF_3] (**3c**) was then isolated analogously to **3a** as an orange solid (0.120 g; 0.168 mmol; 49%). Anal. Calcd for $C_{45}H_{43}F_3P_2Fe$·$C_4H_{10}O$: C, 70.95; H, 6.08; F, 7.16. Found: C, 70.27; H, 5.77; F, 6.90. MS (positive LSI, 3-NBA): *m*/*z* 759 ([**3c**,H]$^+$, 100%); 682 ([(dppe)FeC≡C(C_6H_4)CF_3]$^+$, 5%); 589 ([(dppe)(C_5Me_5)Fe]$^+$, 80%). FT-IR (ν, KBr/Nujol, cm^{-1}): 2053 (s, C≡C); 2028 (sh, C≡C). ^{31}P NMR (δ, C_6D_6, 81 MHz): 101.2 (s, 2P, dppe). ^{19}F-{^{1}H} NMR (δ, C_6D_6, 188 MHz): −61.5 (m, CF_3). ^{1}H NMR (δ, C_6D_6, 200 MHz): 7.88 (m, 4H, H_o(Ar/dppe)); 7.40−6.90 (m, 20H, *H*(Ar/dppe) + *H*($ArCF_3$)); 2.54 (m, 2H, CH_2(dppe)); 1.78 (m, 2H, CH_2(dppe)); 1.47 (s, 15H, C_5(CH_3)$_5$). ^{13}C{^{1}H} NMR (δ, C_6D_6, 50 MHz): 148.2 (t, $^2J_{CP}$ = 39 Hz, Fe−*C*≡C); 140.0−125.0 (m, 8*C*(Ar/dppe) + *C*-H_m($ArCF_3$)+ C≡C−*C*($ArCF_3$)); 125.9 (q, $^1J_{CF}$ = ca. 272 Hz, C_{Ar}−CF_3), 125.4 (q, $^3J_{CF}$ = ca. 4 Hz, *C*−H_o-($ArCF_3$)); 124.3 (q, $^2J_{CF}$ = ca. 37 Hz, C_{Ar}−CF_3); 120.5 (s, Fe−C≡*C*); 88.2 (s, C_5(CH_3)$_5$); 31.1 (m, CH_2(dppe)); 10.5 (s, $^1J_{CH}$ = 126 Hz, C_5(*C*H_3)$_5$).

(η^2-dppe)(η^5-C_5Me_5)Fe[C≡C-1,4-(C_6H_4)Br] (3d). The reaction was run as described for **3c** with 2 equiv of *p*-dibromobenzene (0.150 g; 0.650 mmol). The desired complex (η^2-dppe)(η^5-C_5Me_5)Fe[C≡C-1,4-(C_6H_4)Br] (**3d**) was isolated analogously to **3c** as a pale orange solid (0.180 g; 0.234 mmol; 72%). MS (positive LSI, 3-NBA): *m*/*z* 769 ([**3d**,H]$^+$, 40%); 633 ([(dppe)FeC≡C(C_6H_4)Br]$^+$, 2%); 589 ([(dppe)(C_5Me_5)Fe]$^+$, 100%). FT-IR (ν, KBr/Nujol, cm^{-1}): 2053 (s, C≡C). ^{31}P NMR (δ, C_6D_6, 81 MHz) 101.4 (s, 2P, dppe). ^{1}H NMR (δ, C_6D_6, 200 MHz): 7.92 (m, 4H, H_o(Ar/dppe)); 7.30−6.80 (m, 20H, *H*(Ar/dppe) + *H*(ArBr)); 2.54 (m, 2H, CH_2(dppe)); 1.80 (m, 2H, CH_2(dppe)); 1.50 (s, 15H, C_5(CH_3)$_5$). ^{13}C{^{1}H} NMR (δ, $CDCl_3$, 50 MHz): 142.2 (t, $^2J_{CP}$ = 39 Hz, Fe−*C*≡C); 140.3−125.0 (m, 8*C*(Ar/dppe) + 2*C*−H(ArBr) + C_{quat}(ArBr)); 119.5 (t, $^3J_{CP}$ = ca. 3 Hz, Fe−C≡*C*); 116.3 (s, $^2J_{CH}$ = 11 Hz, C_{quat}(ArBr)); 88.0 (s, C_5(CH_3)$_5$); 30.8 (m, CH_2(dppe)); 10.5 (s, $^1J_{CH}$ = 126 Hz, C_5(*C*H_3)$_5$).

(η^2-dppe)(η^5-C_5Me_5)Fe[C≡C-1,4-(C_6H_4)F] (3e). The reaction was conducted analogously to **3d** with 2.5 equiv of *p*-bromofluorobenzene (0.090 mL; 0.812 mmol), and the desired complex (η^2-dppe)(η^5-C_5Me_5)Fe[C≡C-1,4-(C_6H_4)F] (**3e**) was isolated as an orange solid (0.172 g; 0.243 mmol; 74%). Deep orange crystalline plates could be grown by slow diffusion of pentane into a dichloromethane solution of **3e** (layer/layer).

(76) Connelly, N. G.; Geiger, W. E. *Chem. Rev.* **1996**, *96*, 877−910.
(77) Greenwood, N. N. *Mössbauer Spectroscopy*; Chapman and Hall: London, 1971.

Downloaded by NORTH CAROLINA CONSORTIUM on June 29, 2009
Published on September 9, 2000 on http://pubs.acs.org | doi: 10.1021/om000325o

Downloaded by NORTH CAROLINA CONSORTIUM on June 29, 2009
Published on September 9, 2000 on http://pubs.acs.org | doi: 10.1021/om000325o

MS (positive LSI, 3-NBA): *m*/*z* 709 ([**3e**,H]$^+$, 35%); 589 ([(dppe)(C_5Me_5)Fe]$^+$, 100%); 573 ([(dppe)FeC≡C(C_6H_4)F]$^+$, 2%). FT-IR (*ν*, KBr/Nujol, cm^{-1}): 2056 (s, C≡C). ^{31}P NMR (*δ*, C_6D_6, 81 MHz): 101.7 (s, 2P, dppe). ^{19}F{^{1}H} NMR (*δ*, C_6D_6, 188 MHz): −119.2 (s, C_6H_4F). ^{1}H NMR (*δ*, C_6D_6, 200 MHz): 7.97 (m, 4H, H_o(Ar/dppe)); 7.45−6.90 (m, 18H, *H*(Ar/dppe) + H_o(ArF)); 6.80 (m, 2H, H_m(ArF); 2.60 (m, 2H, CH_2(dppe)); 1.83 (m, 2H, CH_2-(dppe)); 1.53 (s, 15H, C_5(CH_3)$_5$). ^{13}C{^{1}H} NMR (*δ*, C_6D_6, 50 MHz): 160.2 (d, $^1J_{CF}$ = 241 Hz, F−*C*(ArF)); 136.9 (t, $^2J_{CP}$ = ca. 39 Hz, Fe−*C*≡C); 140.6−127.4 (m, 8*C*(Ar/dppe) + 2*C*−H(ArF) + C_{quat}(ArF)); 118.8 (t, $^2J_{CP}$ = ca. 3 Hz, Fe−C≡*C*); 115.2 (d, $^2J_{CF}$ = 22 Hz, *C*-H_o(ArF)); 87.9 (s, C_5(CH_3)$_5$); 30.7 (m, *C*H_2-(dppe)); 10.6 (s, $^1J_{CH}$ = 126 Hz, C_5(*C*H_3)$_5$).

(η²-dppe)(η⁵-C₅Me₅)Fe[C≡C−(C₆H₅)] (3f). The reaction was effected as described for **3b** with 5 equiv of bromobenzene (0.171 mL; 1.625 mmol). The desired complex (η²-dppe)(η⁵-C_5-Me_5)Fe[C≡C-1,4-(C_6H_6)] (**3f**) was isolated analogously to **3a** as an orange solid (0.159 g; 0.231 mmol; 71%) and identified by comparison of its spectral characteristics with those of an authentic sample of **3f** isolated by the reported procedure.[24] Crystals of **3f**·C_5H_{12} were grown by slowly cooling (−40 °C) a solution of the complex in a *n*-pentane−toluene mixture. MS (positive LSI, 3-NBA): *m*/*z* 691 ([**3f**,H]$^+$, 85%); 589 ([(dppe)-(C_5Me_5)Fe]$^+$, 100%); 555 ([(dppe)FeC≡C(C_6H_5)]$^+$, 5%).

(η²-dppe)(η⁵-C₅Me₅)Fe[C≡C(C₆H₄)Me] (3g). The reaction was effected analogously to **3c** with 5 equiv of *p*-bromotoluene (0.205 mL; 1.625 mmol), and the desired complex (η²-dppe)(η⁵-C_5Me_5)Fe[C≡C-1,4-(C_6H_4)Me] (**3g**) was isolated as an orange solid (0.155 g; 0.220 mmol; 70%). Orange crystals can be grown by slow diffusion of pentane in a dichloromethane solution of **3g** (layer/layer). MS (positive LSI, 3-NBA): *m*/*z* 704 ([**3g**]$^+$, 40%); 589 ([(dppe)(C_5Me_5)Fe]$^+$, 100%); 569 ([(dppe)Fe-C≡C(C_6H_4)Me]$^+$, 5%). FT-IR (*ν*, KBr/Nujol, cm^{-1}): 2062 (s, C≡C). ^{31}P NMR (*δ*, C_6D_6, 81 MHz): 101.8 (s, 2P, dppe). ^{1}H NMR (*δ*, C_6D_6, 200 MHz): 8.05 (m, 4H, H_o(Ar/dppe)); 7.30−6.90 (m, 20H, *H*(Ar/dppe) + *H*(ArMe)); 2.65 (m, 2H, CH_2(dppe)); 2.14 (s, 3H, CH_3); 1.86 (m, 2H, CH_2(dppe)); 1.55 (s, 15H, C_5(CH_3)$_5$). ^{13}C{^{1}H} NMR (*δ*, C_6D_6, 75 MHz): 134.7 (t, $^2J_{CP}$ = 40 Hz, Fe-*C*≡C); 140.0−127.0 (m, 8*C*(Ar/dppe) + 2 *C*−H(ArMe) + 2 C_{quat}-(ArMe)); 120.3 (t,$^2J_{CP}$ = 2 Hz, Fe−C≡*C*); 86.6 (s, C_5(CH_3)$_5$); 29.9 (m, *C*H_2(dppe)); 20.1 (s, $^1J_{CH}$ = 126 Hz, C_{Ar}−*C*H_3); 9.3 (s, $^1J_{CH}$ = 126 Hz, C_5(*C*H_3)$_5$).

(η²-dppe)(η⁵-C₅Me₅)Fe[C≡C-1,4-(C₆H₄)ᵗBu] (3h). The coupling was started as described previously from complex **1** (0.300 g, 0.489 mmol) and 2 equiv *p*-*tert*-butylbromobenzene (0.160 mL; 0.960 mmol). After cryogenic trapping of the amine the residual solid was dried (the yield of the desired (η²-dppe)(η⁵-C_5Me_5)Fe[C≡C-1,4-(C_6H_4)^{t}Bu] (**3h**) complex is 65% by NMR). Then it was redissolved in 20 mL of toluene and the solution filtered on a Celite pad, after which the solvent was evaporated. The brown residue (0.255 g) was next dissolved in dichloromethane, oxidized with [Fe(η⁵-C_5H_5)$_2$$^+$][$PF_6^-$] (0.083 g; 0.250 mmol), and precipitated by addition of diethyl ether (see later for related oxidations). After isolation by decantation and drying in vacuo, the green salt that precipitated, [(η²-dppe)(η⁵-C_5Me_5)Fe{C≡C-1,4-(C_6H_4)^{t}Bu}$^+$][PF_6^-] (**3h**$^+PF_6^-$), was immediately redissolved in dichloromethane and reduced back to the starting complex with Co(η⁵-C_5H_5)$_2$ (0.037 g; 0.191 mmol). Extraction in diethyl ether yielded the desired neutral complex **3h** as a bright orange solid after vacuum-drying (0.145 g; 0.191 mmol; 40%). Anal. Calcd for $C_{48}H_{52}P_2Fe$: C, 77.21; H, 7.02. Found: C, 76.74; H, 6.95. MS (positive LSI, 3-NBA): *m*/*z* 747 ([**3h**,H]$^+$, 45%); 589 ([(dppe)(C_5Me_5)Fe]$^+$, 100%). FT-IR (*ν*, KBr/Nujol, cm^{-1}): 2055 (s, C≡C). ^{31}P NMR (*δ*, C_6D_6, 81 MHz) :101.8 (s, 2P, dppe). ^{1}H NMR (*δ*, C_6D_6, 200 MHz): 8.06 (m, 4H, H_o(Ar/dppe)); 7.30−7.00 (m, 20H, *H*(Ar/dppe) + *H*(Ar-^{t}Bu)); 2.69 (m, 2H, CH_2(dppe)); 1.85 (m, 2H, CH_2(dppe)); 1.55 (s, 15H, C_5(CH_3)$_5$); 1.26 (s, 9H, C(CH_3)$_3$). ^{13}C{^{1}H} NMR (*δ*, CD_2Cl_2, 50 MHz): 145.7(s, C_{quat}(Ar^{t}Bu)); 140.5−120.5 (m, 8*C*(Ar/dppe) + Fe−*C*≡C + 2 *C*−H(Ar^{t}Bu) + 1 C_{quat}(Ar^{t}Bu)); 120.3 (s, Fe−C≡*C*); 87.8 (s, C_5(CH_3)$_5$); 34.5 (s, *C*(CH_3)$_3$); 31.7 (s, $^1J_{CH}$ = 125 Hz, C(*C*H_3)$_3$); 30.9 (m, *C*H_{2dppe}); 10.6 (s, $^1J_{CH}$ = 126 Hz, C_5(*C*H_3)$_5$).

(η²-dppe)(η⁵-C₅Me₅)Fe[C≡C-1,4-(C₆H₄)OMe] (3i). The coupling was started as described for **3c** with 2.5 equiv of 4-iodoanisole (0.130 mL, 0.812 mmol). After 12 and 18 h total reaction time, additional portions of palladium catalyst were added (2 × 0.023 g, 2 × 0.032 mmol), after which the heating was maintained further over 12 h. Subsequent isolation of the product is similar to that previously described for **3i** after cryogenic trapping of the amine, using [Fe(η⁵-C_5H_5)$_2$$^+$][$PF_6^-$] (0.037 g; 0.111 mmol) and Co(η⁵-C_5H_5)$_2$ (0.016 g; 0.085 mmol). The desired complex (η²-dppe)(η⁵-C_5Me_5)Fe[C≡C-1,4-(C_6H_4)-OMe] (**3i**) was obtained as a bright orange solid (0.071 g; 0.099 mmol; 30%). Anal. Calcd for $C_{45}H_{46}P_2OFe$: C, 75.00; H, 6.43. Found: C, 75.03; H, 6.16. MS (positive LSI, 3-NBA): *m*/*z* 720 ([**3i**]$^+$, 55%); 589 ([(dppe)(C_5Me_5)Fe]$^+$, 100%); 585 ([(dppe)Fe-C≡C(C_6H_4)OMe]$^+$, 3%). FT-IR (*ν*, KBr/Nujol, cm^{-1}): 2062 (s, C≡C). ^{31}P NMR (*δ*, C_6D_6, 81 MHz): 101.8 (s, 2P, dppe). ^{1}H NMR (*δ*, C_6D_6, 200 MHz) 8.06 (m, 4H, H_o(Ar/dppe)); 7.40−6.90 (m, 18H, *H*(Ar/dppe) + *H*(ArOMe)); 6.82 (d, $^3J_{HH}$ = 8.6 Hz, 2H, *H*(ArOMe)); 3.36 (s, 3H, OCH_3); 2.67 (m, 2H, CH_2(dppe)); 1.84 (m, 2H, CH_2(dppe)); 1.55 (s, 15H, C_5(CH_3)$_5$). ^{13}C{^{1}H} NMR (*δ*, C_6D_6, 75 MHz): 156.7 (s, C_{quat}(ArOMe)); 140.5−127.1 (m, 8*C*(Ar/dppe) + *C*−H(ArOMe)); 131.8 (t, $^2J_{CP}$ = 40 Hz, Fe−*C*≡C); 124.9 (s, $^2J_{CH}$ = 7 Hz, C_{quat}(ArOMe)); 119.4 (t, $^3J_{CP}$ = 3 Hz, Fe−C≡*C*), 114.1 (s, $^1J_{CH}$ = 157 Hz, *C*−H(ArOMe)); 87.5 (s, C_5(CH_3)$_5$); 54.9 (s, $^1J_{CH}$ = 143 Hz, OCH_3); 30.8 (m, *C*H_2-(dppe)); 10.5 (s, $^1J_{CH}$ = 126 Hz, C_5(*C*H_3)$_5$).

(η²-dppe)(η⁵-C₅Me₅)Fe[C≡C-1,4-(C₆H₄)NH₂] (3j). (η²-dppe)(η⁵-C_5Me_5)Fe(Cl) (1.700 g, 2.724 mmol), NH_4PF_6 (0.535 g, 3.282 mmol), and *p*-aminophenylacetylene (0.400 g; 3.419 mmol) were suspended in 100 mL of methanol and the solution was stirred for 12 h at 40 °C. After removal of the solvent, the orange residue was extracted with dichloromethane and the extract concentrated in vacuo. Several washings with diethyl ether yielded the slightly air-sensitive orange complex [(η²-dppe)(η⁵-C_5Me_5)Fe=C=CH{1,4-(C_6H_4)NH_2}$^+$][PF_6^-] (1.775 g; 2.086 mmol; 76%; FT-IR (*ν*, KBr/Nujol, cm^{-1}) 3446, 3364 (m, N−H), 1624 (s, Fe=C=C)). This vinylidene salt (1.600 g; 1.880 mmol) was then stirred for 1 h in THF in the presence of excess potassium *tert*-butylate (0.250 g; 2.212 mmol). After evacuation of the solvent, extraction with toluene, concentration of the extract to dryness, and subsequent washings with *n*-pentane or acetonitrile afforded the desired orange complex (η²-dppe)(η⁵-C_5Me_5)Fe[C≡C-1,4-(C_6H_4)NH_2] (**3j**; 0.745 g; 1.058 mmol; 58%). Anal. Calcd for $C_{44}H_{45}NP_2Fe$: C, 74.89; H, 6.43; N, 1.98. Found: C, 75.48; H, 6.50; N, 2.17. MS (positive LSI, 3-NBA): *m*/*z* 705 ([**3j**]$^+$, 100%); 589 ([(dppe)(C_5Me_5)Fe]$^+$, 47%); 570 ([(dppe)FeC≡C(C_6H_4)NH_2]$^+$, 7%). FT-IR (*ν*, KBr/Nujol, cm^{-1}): 2057 (s, C≡C). ^{31}P NMR (*δ*, C_6D_6, 81 MHz): 102.0 (s, 2P, dppe). ^{1}H NMR (*δ*, C_6D_6, 200 MHz): 8.05 (m, 4H, H_o(Ar/dppe)); 7.40−6.95 (m, 18H, *H*(Ar/dppe) + *H*(ArNH_2)); 6.30 (d, $^3J_{HH}$ = 8.6 Hz, 2H, *H*(ArNH_2)); 2.67 (m, 4H, NH_2 + CH_2(dppe)); 1.82 (m, 2H, CH_2(dppe)); 1.54 (s, 15H, C_5(CH_3)$_5$). ^{13}C{^{1}H} NMR (*δ*, CD_2Cl_2, 75 MHz): 142.7 (s, $^2J_{CH}$ = 9 Hz, C_{quat}(ArNH_2)); 130.9 (t, $^2J_{CP}$ = 40 Hz, Fe−*C*≡C); 139.5−127.1 (m, 8*C*(Ar/dppe)); 131.0 (s, *C*−H(ArNH_2)); 122.6 (s, $^2J_{CH}$ = 8 Hz, C_{quat}(ArNH_2)); 118.7 (s, Fe−C≡*C*); 115.2 (s, $^1J_{CH}$ = 154 Hz, *C*−H(ArNH_2)); 109 (s, C_{quat}(ArNH_2)); 87.7 (s, C_5(CH_3)$_5$); 31.0 (m, *C*H_2(dppe)); 10.3 (s, $^1J_{CH}$ = 126 Hz, C_5(*C*H_3)$_5$).

(η²-dppe)(η⁵-C₅Me₅)Fe−C≡C-1,4-(C₆H₄)NMe₂ (3k). The coupling reaction was started from complex **1** (0.400 g; 0.325 mmol), with the palladium catalyst (0.046 g; 0.032 mmol) and copper iodide cocatalyst (0.026 g; 0.065 mmol), using 4-bromodimethylaniline as the halogenated substrate (0.261 g; 1.305 mmol) in 10 mL of diisopropylamine. After a coupling procedure similar to that used for **3i**, the desired complex (η²-dppe)(η⁵-C_5Me_5)Fe[C≡C-1,4-(C_6H_4)NMe_2] (**3k**) was identified (IR, NMR) admixed with another unknown complex and starting bromoaniline (spectroscopic yield of **3k**: 55%). The

Downloaded by NORTH CAROLINA CONSORTIUM on June 29, 2009
Published on September 9, 2000 on http://pubs.acs.org | doi: 10.1021/om000325o

subsequent use of a redox-based purification protocol similar to the one used previously did not allow isolation of a pure sample of **3k**; however, this complex was largely dominant in the mixture. FT-IR (ν, KBr/Nujol, cm^{-1}): 2056 (s, C≡C). ^{31}P NMR (δ, C_6D_6, 81 MHz) :102.0 (s, 2P, dppe). ^1H NMR (δ, C_6D_6, 200 MHz): 8.09 (m, 4H, H_o(Ph1/dppe)); 7.40−6.90 (m, 18H, *H*(Ar/dppe) + *H*($ArNMe_2$)); 6.65 (d, $^3J_{HH}$ = 8.8 Hz, 2H, *H*($ArNMe_2$)); 2.65 (m, 4H, NH_2 + CH_2(dppe)); 2.56 (s, 3H, $N(CH_3)_2$); 1.82 (m, 2H, CH_2(dppe)); 1.54 (s, 15H, $C_5(CH_3)_5$). $^{13}C\{^1H\}$ NMR (δ, C_6D_6, 50 MHz): 149.8 (s, C_{quat}($ArNMe_2$)); 140.3−127.0 (m, 8*C*(Ar/dppe) + Fe−*C*≡C); 123.3 (s, $^1J_{CH}$ = ca. 156 Hz, *C*−H($ArNMe_2$)); 120.5 (s, C_{quat}($ArNMe_2$)); 120.0 (s, Fe−C≡*C*); 113.7 (s, $^1J_{CH}$ = ca. 157 Hz, $^3J_{CH}$ = 4 Hz, *C*−H($ArNMe_2$)); 87.9 (s, $C_5(CH_3)_5$); 41.0 (s, $^1J_{CH}$ = 134 Hz, $^3J_{CH}$ = 4 Hz, $N(CH_3)_2$); 31.1 (m, CH_2(dppe)); 10.6 (s, $^1J_{CH}$ = 126 Hz, $C_5(CH_3)_5$).

[(η^2-dppe)(η^5-C_5Me_5)Fe{C≡C-1,4-(C_6H_4)NO_2}$^+$][PF_6^-]-(3a$^+PF_6^-$). A 0.95 equiv amount of [Fe(η^5-C_5H_5)$_2^+$][PF_6^-] (0.120 g; 0.361 mmol) was added to a solution of **3a** (0.280 g; 0.380 mmol) in 15 mL of dichloromethane, resulting in an instantaneous darkening of the solution. Stirring was maintained for 1 h at room temperature, and the solution was concentrated in vacuo to approximately 5 mL. Addition of 50 mL of *n*-pentane allowed precipitation of a dark orange solid. Decantation and subsequent washing with 3 × 3 mL portions of toluene followed by 3 × 3 mL of diethyl ether and drying under vacuum yielded the pure complex [(η^2-dppe)(η^5-C_5Me_5)Fe{C≡C-1,4-(C_6H_4)NO_2}$^+$][PF_6^-] (**3a**$^+PF_6^-$) as a pale brown solid (0.300 g; 0.340 mmol; 94%). Crystals could be grown by slow diffusion of diethyl ether in a dichloromethane solution of **3a**$^+PF_6^-$·$C_4H_{10}O$ (layer/layer). Anal. Calcd for $C_{44}H_{43}F_6NO_2P_3Fe$: C, 60.02; H, 4.92; N, 1.59. Found: C, 60.03; H, 5.13; N, 1.64. FT-IR (ν, KBr/Nujol, cm^{-1}): 2030 (w, C≡C). UV−vis (λ_{max}, nm (ϵ, 10^{-3} M^{-1} cm^{-1}), CH_2Cl_2): 267 (sh, 85.4); 310 (sh, 16.1); 379 (15.4); 504 (sh, 2.3); 562 (sh, 1.6); 650 (1.2).

[(η^2-dppe)(η^5-C_5Me_5)Fe{C≡C-1,4-(C_6H_4)NH_2}$^+$][PF_6^-] (3j$^+$-PF_6^-). A 0.92 equiv amount of [Fe(η^5-C_5H_5)$_2^+$][PF_6^-] (0.082 g; 0.247 mmol) was added to a solution of **3j** (0.190 g, 0.269 mmol) in 15 mL of dichloromethane at −70 °C. Stirring was maintained for 4 h at this temperature, and the solution was concentrated in vacuo to approximately 5 mL. Addition of 50 mL of precooled *n*-pentane allowed precipitation of a solid. Decantation and subsequent washing with 3 × 3 mL portions of toluene at −70 °C followed by 3 × 3 mL of diethyl ether and drying under vacuum yielded 0.166 g of the desired complex [(η^2-dppe)(η^5-C_5Me_5)Fe{C≡C-1,4-(C_6H_4)NH_2}$^+$][PF_6^-] (**3j**$^+PF_6^-$) as a dark brown solid (0.184 g, 0.215; 80%). Anal. Calcd for $C_{44}H_{45}F_6NP_3Fe\cdot{}^1/_2C_5H_{12}$: C, 62.99; H, 5.80; N, 1.58. Found: C, 63.16; H, 5.48; N, 1.54. FT-IR (ν, KBr/Nujol, cm^{-1}): 1983 (sh, C≡C), 1958 (vs, C≡C). UV−vis (λ_{max}, nm (ϵ, 10^{-3} M^{-1} cm^{-1}), CH_2Cl_2): 268 (sh, 34.5); 287 (8.8); 413 (sh, 6.0); 789 (9.7).

Crystallography. Crystals of **3a**,**b**, **3f**·C_5H_{12}, and **3a**$^+PF_6^-$·$C_4H_{10}O$ were obtained as described above, and the corresponding data are summarized in Table 4. Cell constants and orientation matrices for data collection were obtained from a least-squares refinement using 25 high-θ reflections. For all compounds, after Lorentz and polarization corrections,[78] the structures were solved with SIR-97,[79] which revealed many non-hydrogen atoms of the molecules. The remaining ones were found after anisotropic refinements by a Fourier difference map. The entire structures were then refined with SHELXL97,[80] by full-matrix least-squares techniques (use of *F* magnitude; *x*, *y*, *z*, β_{ij} for Fe, P, N, O and C atoms, and *x*, *y*, *z* in riding mode for H atoms with variables (*N*(var)), observations and "*w*" used as defined in Table 4). Atomic scattering factors were taken from the literature.[81] A Silicon Graphics Indy computer with the MOLEN package (ENRAF-Nonius, 1990) was used for structure determination.[82] ORTEP views of **3a**, **3b**, **3f**·C_5H_{12}, and **3a**$^+PF_6^-$·$C_4H_{10}O$ were realized with PLATON98.[83] All the calculations were performed on a Pentium NT Server computer.

Acknowledgment. We thank S. Le Stang, G. Le Gland, J. Courmarcel, and P. Jéhan (CRMPO, Rennes, France) for experimental assistance. The CNRS is acknowledged for financial support.

Supporting Information Available: A figure giving the ^{31}P NMR (dppe singlet) vs ^1H NMR (C_5Me_5 singlet) correlation for **3a**−**j** in ppm and X-ray structural information for **3a**$^+PF_6^-$·$C_4H_{10}O$, **3a**,**b**, and **3f**·C_5H_{10}, including tables of atomic positional parameters, bond distances and angles, and anisotropic and isotropic thermal displacement parameters. This material is available free of charge via the Internet at http://pubs.acs.org.

OM000325O

(78) Spek, A. L. HELENA: Program for the Handling of CAD4-Diffractometer Output SHELX(S/L); Utrecht University, Utrecht, The Netherlands, 1997.
(79) Altomare, A.; Burla, M. C.; Camalli, M.; Cascarano, G.; Giacovazzo, C.; Guagliardi, A.; Moliterni, A. G. G.; Polidori, G.; Spagna, R. *J. Appl. Chem.* **1998**, *31*, 74−77.
(80) Sheldrick, G. M. SHELX97: Program for the Refinement of Crystal Structures; University of Göttingen, Göttingen, Germany, 1997.
(81) *International Tables for X-ray Crystallography*; Kluwer Academic: Dordrecht, The Netherlands, 1992; Vol. C.
(82) Fair, C. K. MolEN. An Interactive Intelligent System for Crystal Structure Analysis; ENRAF-Nonius, Delft, The Netherlands, 1990.
(83) Spek, A. L. PLATON.: A Multipurpose Crystallographic Tool; Utrecht University, Utrecht, The Netherlands, 1998.
(84) Lichtenberger, D. L.; Rai-Chaudhuri, A. *J. Am. Chem. Soc.* **1991**, *113*, 2923−2930.
(85) Marshall, W. J.; Thorn, D. L.; Grushin, V. V. *Organometallics* **1998**, *17*, 5427−5430.
(86) Lichtenberger, D. L.; Renshaw, S. K.; Bullock, R. M. *J. Am. Chem. Soc.* **1993**, *115*, 3276−3285.
(87) Masai, H.; Sonogashira, K.; Hagihara, N. *J. Organomet. Chem.* **1971**, *26*, 271−276.
(88) Wojtkowiak, B.; Queniec, R. *C. R. Acad. Sci. Paris* **1966**, *262*, 811−814.
(89) de Angelis, F.; Re, N.; Rosi, M.; Sgamellotti, A.; Floriani, C. *J. Chem. Soc., Dalton Trans.* **1997**, 3841−3844.
(90) Le Narvor, N.; Lapinte, C. *J. Chem. Soc., Chem. Commun.* **1993**, 357−359.
(91) Bartik, T.; Dembinski, R.; Bartik, B.; Arif, A. M.; Gladysz, J. A. *New J. Chem.* **1997**, *21*, 739−750.
(92) Grindley, T. B.; Johnson, K. F.; Katritzky, A. R.; Keogh, H. J.; Thirkettle, C.; Brownlee, R. T. C.; Munday, J. A.; Topsom, R. D. *J. Chem. Soc., Perkin Trans. 2* **1974**, 276−282.